

## Shear Behavior of Random Rockfill in Dam Construction via Large-Scale In-Situ Testing

Andhika Sahadewa<sup>1\*</sup>, Abi M. Hakim<sup>2,3</sup>, Haris E. Setyawan<sup>1</sup>,  
Samira A. Kamaruddin<sup>2</sup>, Sugeng Krisnanto<sup>1</sup>

<sup>1</sup>Geotechnical Engineering Research Group, Faculty of Civil and Environmental Engineering, Institut Teknologi Bandung, Bandung, 40132, Indonesia.

<sup>2</sup>Razak Faculty of Technology and Informatics, Universiti Teknologi Malaysia, Kuala Lumpur, 54100, Malaysia.

<sup>3</sup>Department of Civil Engineering, Institut Teknologi Indonesia, South Tangerang, 15314, Indonesia.

Received 29 January 2025; Revised 25 March 2025; Accepted 23 April 2025; Published 01 June 2025

### Abstract

Dam construction commonly demands a massive amount of random material. This material offers practical material collection, minimum environmental impact, and economical cost. Unfortunately, shear strength assessment of random material is difficult because of large particle presence. Regular laboratory tests cannot accommodate these large particles. Misvaluation of random material shear strength may induce disastrous collapse. A large-scale direct shear apparatus, with a 70 cm by 70 cm shear plane, was developed and proposed for testing random fill material in-situ. This manuscript presents an experimental study using this device in Rukoh Dam construction, Indonesia. Test results captured variations between normal stress and shear stress to determine shear strength parameter models. Volume changes during shearing were also observed. Random materials in Rukoh Dam could be categorized as random rock. This study was also compared to other relevant rockfill studies. The proposed method offers an impressive approach for assessing and verifying the shear strength of compacted random material as well as compaction quality on site. It can be used to decide if the ongoing design and compaction method have to be modified or continued. Since the proposed direct shear test is reliable, fast, simple, and inexpensive, it is strongly recommended for dam construction.

**Keywords:** Direct Shear Test; Shear Strength; In-Situ Test; Field Test; Dam; Large-Scale Test; Embankment; Random Materials; Rockfill.

### 1. Introduction

A dam provides many benefits, such as water supply reliability, flood control, hydropower energy, and sailing. These advantages attract many countries to build dams. A dam is commonly built as a homogeneous or zoned embankment dam in developing countries, including Indonesia (Figure 1). A zoned embankment dam comprises several zones where a certain geomaterial type can be deposited in a particular zone. A zoned embankment dam design can be governed by economic considerations as well as geomaterial availability. If a type of geomaterial can satisfy the requirements for stability as well as seepage control, this geomaterial can be selected and placed in a zone to achieve the most affordable design that meets all technical requirements. Thus, a zoned dam body promotes a better utilization of adjacent available geomaterials [1]. A zoned embankment dam can have specific zones for placing random materials. Random material is practically described as geomaterial that is formed naturally or artificially from a variety of constituent types and sizes,

\* Corresponding author: [sahadewa@itb.ac.id](mailto:sahadewa@itb.ac.id)



<http://dx.doi.org/10.28991/CEJ-2025-011-06-03>



© 2025 by the authors. Licensee C.E.J, Tehran, Iran. This article is an open access article distributed under the terms and conditions of the Creative Commons Attribution (CC-BY) license (<http://creativecommons.org/licenses/by/4.0/>).

ranging from clay to boulders in various degrees of weathering. These composite materials are commonly obtained from borrowed materials as well as dam excavation works. Random material can occur by nature (e.g., moraine or till and river deposit) or be manmade (e.g., crushed rock sand). In a dam design, random fill zones become a crucial factor in minimizing the construction cost. As it is named random material, a wide range of geomaterial types, sizes, and weathering stages can be used. Thus, competitive geomaterials from any quarries as well as remaining geomaterials from excavation generally can be included to reach the required fill volume. Flexible selection in random material constituents is one of the contributive points in reducing environmental disturbances.

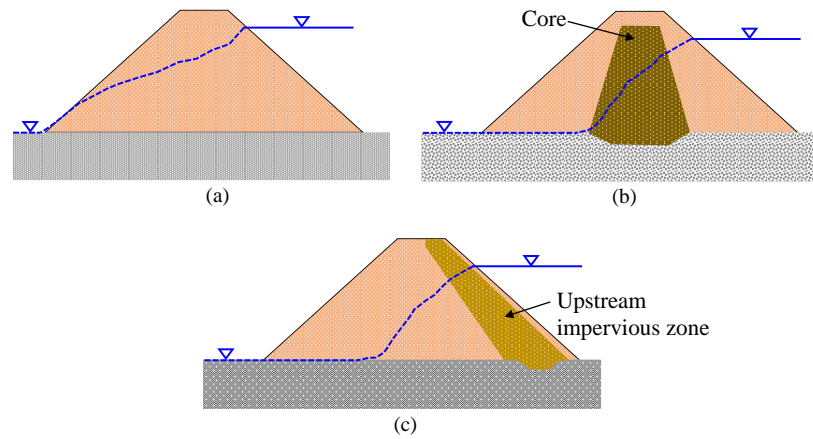


**Figure 1. Embankment dams: (a) homogenous, (b) with core zone, and (c) with upstream impervious zone**

Random material leads to embankment work challenge despite its benefits. A wide range of material types and sizes in random materials may introduce very large spatial variability of material properties in random fill zones, including the shear strength. In particular, slope instability can occur in random fill zones. X Dam construction in Indonesia emphasized random material fill failure case. Three consecutive landslides occurred in the downstream of X Dam (Figure 2). Interested readers are suggested to read Sahadewa et al. [2] for the details of the X Dam slope instability accident, forensic investigation, and mitigation measures.

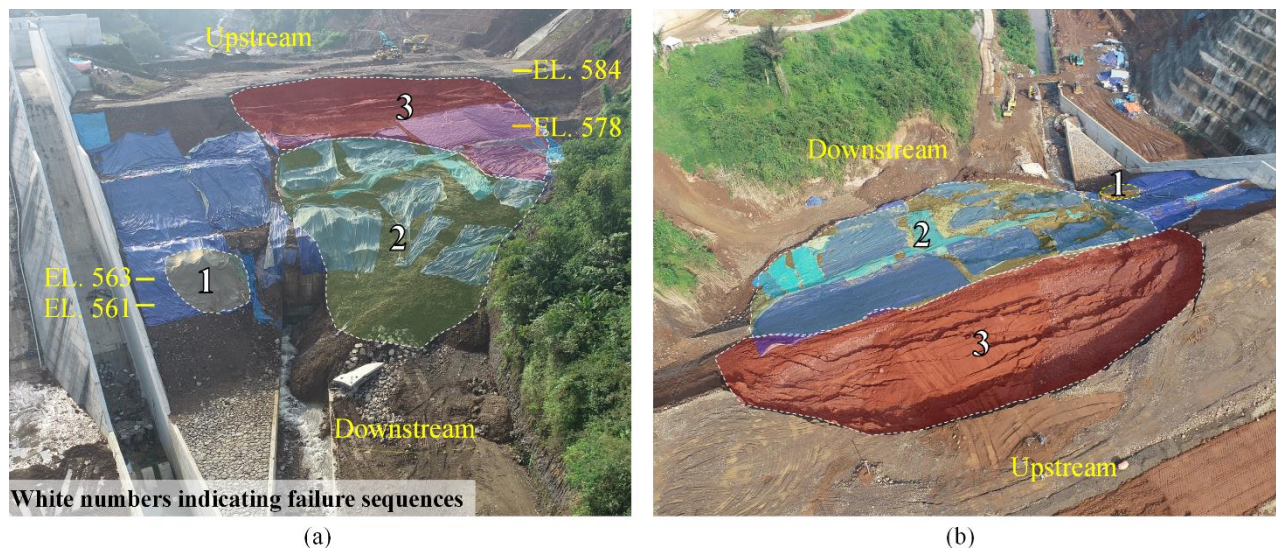


**Figure 2. X Dam slope failure accident: (a) downstream and (b) upstream views [2]**

A reliable method for shear strength appraisal of random material was urgently required in ongoing dam construction in Indonesia since the X Dam incident. Yet, evaluating this shear strength is difficult. Random materials often contain large-sized particles that impede the application of standard-sized field and laboratory tests. Field and laboratory large-scale direct shear testing on various materials consisting of large-size particles has gained popularity for more than 2 decades. Liu [3] and Matsuoka et al. [4] proposed a new large-scale direct shear apparatus for testing granular embankment materials on site. A set of large-scale laboratory tests using specimen lengths of 50 cm and 100 cm were conducted for evaluating shear strength properties of loose accumulated soils associated with the 2008 Sichuan earthquake by Wang et al. [5]. In more recent years, large-scale direct shear devices were applied for testing a variety of materials. Shear strength properties of rock in the dam foundation were evaluated using a large-scale field direct shear

test by Sagnak et al. [6]. Zhang et al. [7] studied the influences of sand fouling and coal fines on the shear strength of railway ballast by applying laboratory direct shear with sample dimensions of 40 cm × 40 cm × 40 cm. Wang et al. [8] evaluated the railway ballast degradation using a laboratory direct shear device with a 60 cm × 40 cm shear plane. Large-scale laboratory direct shear was utilized to investigate wetland soil-root matrix shear strength by Hassan et al. [9]. Large-scale direct shear is also attractive for assessing soil reinforcement interface shear strength. Chao et al. [10] studied the interface strength between various geosynthetic materials with silica sand by applying a large-scale direct shear device with a shear plane of 30 cm × 30 cm. A large-scale direct shear device having a 30.5 cm by 30.5 cm shear plane was used by Chen et al. [11] to study the coral sand-geogrid interface. Despite these recent studies, equivalent shear strength testing on random material in large dam construction is still rarely found in the literature.

An in-situ or field large-scale test is appealing to firmly evaluate the shear strength of dam construction materials, such as random fill. Indonesian Geotechnical Institute (IGI), Institut Teknologi Bandung (ITB), and Universiti Teknologi Malaysia (UTM) were in cooperation to develop in situ large-scale direct shear equipment, abbreviated as ILSDS. The in-situ approach was suggested instead of the laboratory counterpart so that the results can also incorporate the actual field compaction effect on the material shear strength. The test was tailored in such a way that preparation and execution could be parallel with dam construction using equipment that is promptly available on the site. Thus, the application of this proposed method is fast, simple, reliable, and inexpensive. As part of the proposed device development, proof-of-concept tests have been successfully executed in several large dam constructions [12-15]. An experimental study in the assessment of shear strength by applying the proposed device on random material in Rukoh Dam, Indonesia, is reported in this article.

This article comprises 5 major parts, namely introduction, main body, concluding paragraph, declaration, and references. The main body consists of the Rukoh Dam description, random material application in dams, the history and concept of the direct shear test, the shear strength of random material, as well as the ILSDS test in Rukoh Dam. The summary, conclusion, and suggestion that can be learned from this study are described in the concluding paragraph.

## 2. Rukoh Dam

Rukoh Dam is located across the Krueng Rukoh River in Pidie, Aceh, Indonesia. This dam was listed in one of Indonesia's strategic national projects in 2016. To enhance the water supply in this dam, a tunnel irrigation channel from the Tiro River to the Rukoh Dam was also constructed. Having an inundation area of around 716.1 ha in normal water level, Rukoh Dam is capable of holding more than 128.66 million m<sup>3</sup> of water. Rukoh Dam was primarily built to provide a water supply of 0.90 m<sup>3</sup>/second for 22,848 people in Pidie. Additionally, this dam was planned to serve a farming area of about 11,950 ha. This dam was also intended for mitigating floods with a 50-year return period in Pidie. This mitigation accounts for reducing Krueng Rukoh River floods as large as 89.62%. In addition, Rukoh Dam has the potential to facilitate a power plant with a capacity of 1.22 MW.

Rukoh Dam is regionally situated among 3 rock units, namely the Kotabakti formation, the Kotabakti Anggota Pintu Satu formation, and the alluvial formation, from the oldest to the youngest formation, respectively. The Kotabakti formation was formed in the middle of the Miocene period. This formation was composed of interbedded layers of sandy siltstone and claystone. The Kotabakti Anggota Pintu Satu formation comprises interbedded layers of fine to coarse silty sandstone. This formation also occurred in the middle of the Miocene period. The alluvial formation was formed by Krueng Rukoh sedimentation. This formation contains sand, gravel, cobble, and boulder in loose condition.

Rukoh Dam is approximately 87 m high and 220 m long at the peak. Figure 3 presents an example of a Rukoh Dam cross-section. The core inclined 4V:1H. A fine filter layer was placed surrounding the dam core. Random fill zones in Rukoh Dam are indicated by number 4 in Figure 3. The dam body was protected by constructing a riprap layer on the surface.

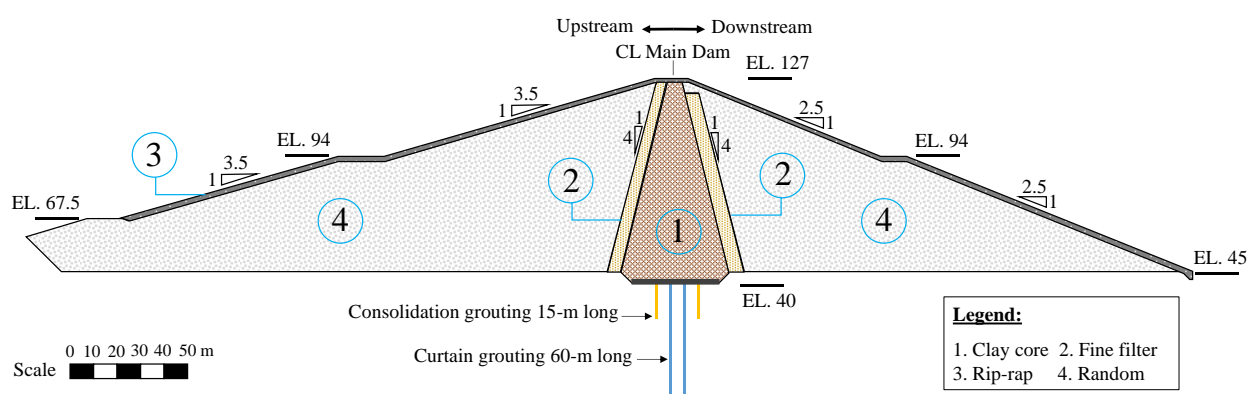


Figure 3. An example of Rukoh Dam cross-section

### 3. Application of Random Fill Material in Dams

Placement of random material is generally associated with less important areas of the dams. The US Bureau of Reclamation, or USBR [16], recommended random material use in dam zones where the major requirement is geomaterial weight. In this case, the main concern does not include permeability and shear strength of the geomaterials. The USBR [16] also presented an example of random material application in the interior and exterior zones (Figures 4 and 5). In the exterior zone, random material is applied to build: (1) counterweight to increase stability (Figure 4-a) and (2) flat slope to reduce slope protection (Figure 4-b). In the interior zone, random material is placed inside the supporting dam shell to minimize material cost (Figure 5).

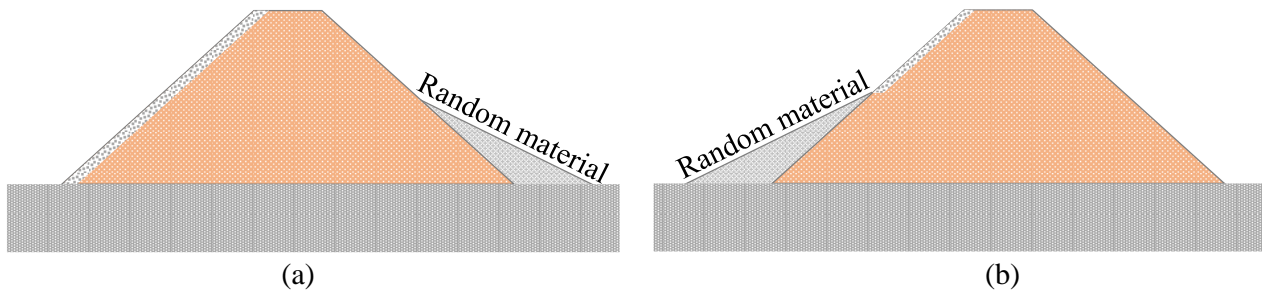


Figure 4. Examples of random fill material in exterior of dam: (a) counterweight and (b) slope protection reduction [16]

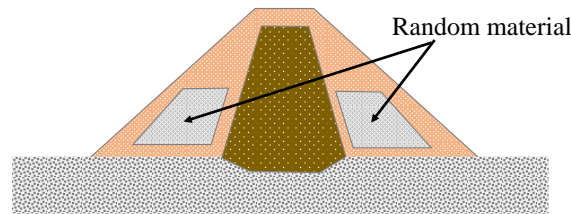


Figure 5. An example of random fill material in interior of dam [16]

The US Society on Dams, or USSD [17], described the use of random fill for constructing one of the common main elements in the Concrete Facing Rockfill Dam (CFRD). The random fill is normally constructed in an upstream fill to protect the perimeter joint. This random material serves to seal any cracks that may develop around the perimeter joint in the lower elevations of dams higher than 75 m. The random fill may consist of a variety of soil sizes, including clay, silt, sand, and gravel. This geomaterial can cover and provide sufficient weight for underlain material to allow it to penetrate the cracks [17].

Application of random material is also recommended in the dam's vital areas. For instance, the International Commission on Large Dams, or ICOLD [18], presented a comprehensive review of understanding and experience in using moraine (i.e., random material) as a dam foundation and fill material. According to ICOLD [18], the particle size distribution and composition of moraine are commonly related to the source rocks and the soils below the glacier move. Granitic gneiss, granite, and identical large and hard rocks formed till containing sandy silt skeletons. Softer sedimentary rocks, namely shale and limestone, formed clayey skeletons. Furthermore, ICOLD [18] stated that, if moraine is sufficiently impervious, it could be utilized for dam cores and homogeneous earth dams.

Case histories of random material application in a dam core construction are reported in the literature. Sherard and Dunnigan [19] described glacial moraine utilization to build the dam's impervious section. They categorized the entire range of soils for impervious sections into 4 soil groups, namely (1) fine silts and clay or > 85% fine materials, (2) silty sand, clayey sand, sandy silt, and sandy clays or 40%–85% fine materials, (3) silty sand, clayey sand, and gravelly sand or ≤ 15% fine materials, and (4) soil intermediate between Groups 2 and 3. In these groups, fine materials were passing the No. 200 sieve. Concentrated leaks through impervious sections of embankment dams could be reliably controlled and sealed using sand filters containing the proper amount of fine sand [19]. Thus, a relatively fine filter is recommended for impervious sections of glacial moraines. Rönnqvist [20] assessed internal erosion of more than 90 dams in Scandinavia, North America, Australia, and New Zealand. The impervious section of these dams was built using broadly graded glacial till materials that belonged to Group 2 of [19]. The Scandinavian glacial tills were generally non-plastic and low-plasticity clay [21]. Glacial till materials applied in Scandinavian dams typically contained 15% to 60% materials passing the No. 200 sieve. Glacial tills used in North American dam cores were relatively fine-rich, with 20% to 70% of materials passing the No. 200 sieve, whereas those of Russian dams were fines-poor, with 5% to 20% passing the No. 200 sieve [18]. Rönnqvist [20] suggested that, when assessing the potential of internal erosion to surface, namely erosion in the excessive or continuing phase, evaluation should not only be performed on the filter's coarseness but also



on the grading stability of the filter and the core material as well as non-homogeneities that were caused by filter segregation. Xu & Jiang [22] reported lessons from using broadly graded geomaterials to build earth core rockfill dams in China. Gradation of soils for constructing the core was advised to be adjusted according to the requirements on strength, permeability, and deformation as well as the conditions of the original borrow materials [22]. Random material containing colluvial and residual soils was used to construct the core of Manso Dam in Brazil, according to Ferreira et al. [23]. The random material of Manso Dam is composed of a blend of colluvial and residual soils from metasiltitic rock and the corresponding fragments in sound or weathered condition. It also included intercalations of quartz and metasandstones. The random fill also contained lateritic topsoil containing clumps of cemented fine-grained soils. The main dam construction utilized around 500,000 m<sup>3</sup> of random materials, or about 30% of the complete Manso Dam. Manmade artificial random fill materials have also been applied to construct dam embankment cores. Ma & Chi [24] presented an insightful experience in blending fine cohesive soils (< 35%) with coarse gravel (50% – 65%) to build a dam core in the Changheba Dam, China. Fu et al. [25] recommended 30%–50% of gravel content in adjusting the gravel-fine soil blend to construct a core of a 200-m to 300-m high dam based on project experiences from Nuozhadu, Pubugou, Lianghekou, and Changheba Dams in China.

Random materials were also used for building the main dam body, excluding the core and fine filter zones. Sahadewa [12] reported random materials application in constructing the main dam body of Semantok Dam, Nganjuk, Indonesia. These materials were placed in the upstream and downstream dam embankments. The random materials were generally volcanic breccia containing a blend of tuff and igneous andesite rock. During compaction works, the random fill materials experienced considerable grain break that reduced the particle size. Random fill materials were also utilized in the upstream as well as downstream of the X Dam [14]. A blend of weathered rocks and colluvial deposits formed these random materials. Lapilli tuffs, agglomerate, and breccia were the primary constituents in the weathered rocks. A variety of geomaterial sizes, ranging from fine cohesive soils to boulders, formed the colluvial deposits. Sahadewa [15] reported random material application in the main body of Kuwil Kawangkoan Dam, North Minahasa, Indonesia. Random material in this dam was random rock that had a similar size to rockfill materials.

Particle size distributions of some random fill materials in dams are presented in Figure 6. For comparison, this figure presents upper and lower bounds of rockfill for dam embankments by Kutzner [26] and Fell et al. [27], respectively. The lower bound of sand-gravel or gravel for CFRD main fill as proposed by Haselsteiner et al. [28] is also shown in this figure. Figure 6 suggests that the particle size range of random materials is broader than that of other geomaterials.

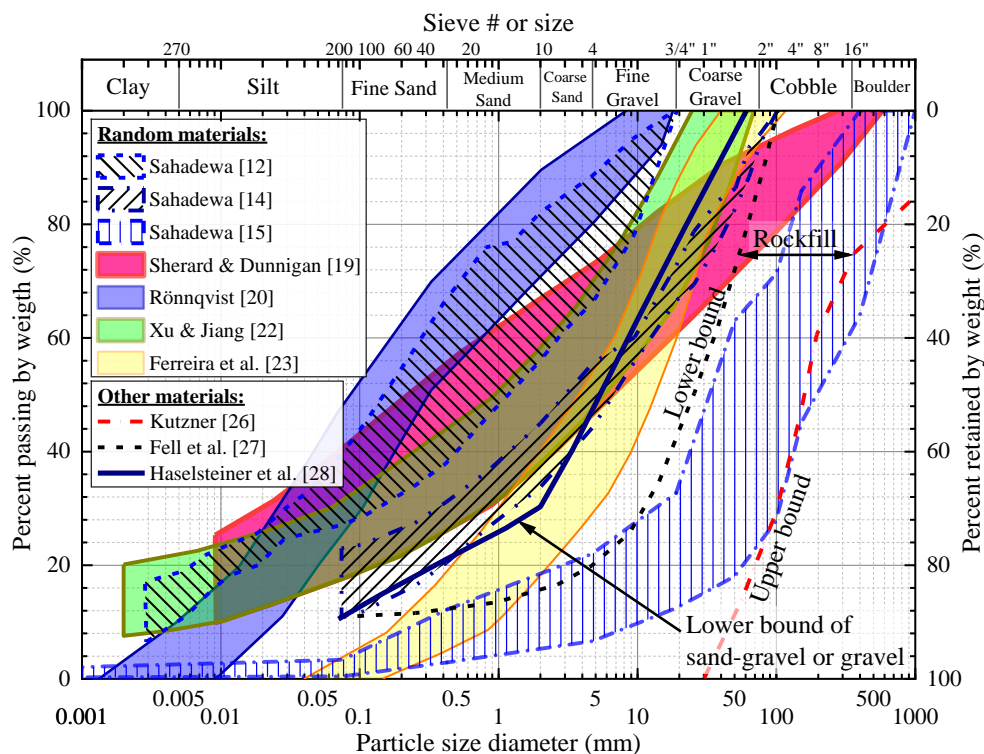


Figure 6. Particle size distribution of various materials in dam construction

One major challenge associated with the utilization of random materials relates to wide variation in homogeneity due to broadly graded particles. Random material has been suggested for construction in less vital areas of the dams, where material's weight is the main concern [16]. In these areas, the permeability as well as shear strength of the random fill materials are mostly not crucial. Thus, the utilization of random fill material in these areas is relatively simple.

Nevertheless, random material utilization is more challenging when the random fill zone covers large parts of the main dam body and dam core, which are prone to instability. Unfortunately, at least in Indonesia, the “random” term itself introduces the misunderstanding that any geomaterials with varying sizes, types, and weathering stages can be included to fulfill the required volume. This mistake may lead to the incorporation of problematic geomaterials, such as expansive soils, organic soils, and low-slaking durability materials, in random materials. In addition, if random material is applied in critical zones, there are many criteria that should be complied with. For example, if random material is used to build a dam core, suffusion risk should be evaluated comprehensively [29, 30]. Suffusion risk is a condition where fine soil particles potentially drift within the coarser soil skeleton or matrix.

Depending on the random material type and random fill zone, certain material requirements must be fulfilled to achieve the expected dam performance. The incident of X Dam was an invaluable lesson on not using random materials carelessly, particularly in dam critical zones. The economical and environmentally friendly benefits of using random material in critical dam zones should be accompanied by comprehensive geotechnical investigations, characterizations, and inspections of random materials. Dam designers and construction teams should comprehend the shear strength, permeability, compressibility, and other essential properties of random materials and the corresponding spatial variability throughout the dam. To achieve these goals and to provide important parameters for dam stability evaluation, in-situ or field large-scale direct shear tests were suggested by the authors to reliably assess and verify the shear strength of compacted random fill materials and other dam construction materials.

#### 4. Direct Shear Test

The direct shear is one of the available tests for evaluating the shear strength of geomaterial. This test is believed to be the first method for assessing soil shear strength according to Boudia et al. [31]. Coulomb is believed by many to be the originator of soil shear strength theory. However, who pioneered the direct shear test equipment is still a matter of debate. Alexandre Collin, a French engineer, developed a direct shear apparatus in 1846 [32]. Collin used a 35-cm-long, 4-cm-wide, and 4-cm-thick shear box for holding a clayey soil sample. In 1915, Arthur Langtry Bell, a British engineer, developed a direct shear device to test various types of soil [33]. In 1932, Arthur Casagrande developed a direct shear device, which became the basis for similar equipment in modern times [34].

Despite the emergence of other testing devices, such as triaxial, to evaluate geomaterial shear strength, the direct shear test remains popular today because of several advantages [35]. These advantages include:

- Testing can be performed quickly and simply.
- Testing cost is economical.
- The soil parameters obtained by direct shear are about as reliable as those of triaxial.
- Shear boxes offer easier preparation of granular soil samples compared to the preparation of such samples in other soil test devices (e.g., triaxial).

Nevertheless, the direct shear test also has commonly known shortcomings, namely:

- Soil pore water drainage control is limited and can only be done by controlling the displacement speed.
- Pore water pressure cannot be measured during testing.
- Displacement is forced to occur in a plane that is not necessarily the weakest shear plane.
- The sample can experience stress concentration in certain parts so that the strain is not uniform.

Many institutions host laboratory-scale direct shear test facilities (Table 1). These shear box sizes are far larger than the commonly available sizes of 6 cm × 6 cm, 10 cm × 10 cm, and 15 cm × 15 cm. Both laboratory regular-scale and large-scale direct shear devices are impressive for parametric studies on the shear strength of geomaterial. Some facilities offer large-scale testing under saturated and dry conditions. However, the prepared geomaterial sample is mostly reconstituted using a laboratory-scale compactor. Hence, the sample may not always represent the field-compacted condition perfectly.

**Table 1. Examples of laboratory large-scale direct shear test facilities**

| Institution  | Area of shearing plane<br>$L$ (cm) × $W$ (cm) | Reference                     |
|--|---|-------------------------------|
| The University of Wales, UK  | 300 × 150                                     | Davies & Le Masurier [36]     |
| Jaroslav Cerni Institute for Development of Water Resources, Serbia                              | 80 × 80                                       | Andjelkovic et al. [37]       |
| City University of London, UK  | 150 × 100                                     | Tanghetti et al. [38]         |
| Indian Institute of Technology, Roorke, India  | 75 × 75                                       | Srivastava et al. [39]        |
| CEDEX, Laboratorio de Geotecnia, Madrid, Spain   | 100 × 100                                     | Muñiz-Menéndez & Estaire [40] |
| River Basin Management Organizations for Bengawan Solo, Ministry of Public Work, Solo, Indonesia | 125 × 125                                     | -                             |

The in-situ, or field, large-scale direct shear test has occurred since 1904 [33]. Examples of large-scale direct shear field tests are listed in Table 2. Similar to other in-situ tests, this type of direct shear test offers testing on an “undisturbed” sample. In some cases, the “undisturbed” sample testing is of interest. For example, in dam embankment construction, the geomaterial is compacted using heavy equipment. This compaction effort may not be replicated in the laboratory. In fact, compaction energy directly influences the shear strength of geomaterials, e.g., [41, 42]. The field of large-scale direct shear becomes more attractive if the compacted geomaterial consists of larger particles. Application of large-scale direct field shear for testing random dam material is rare in the literature, despite many having performed this method on other materials.

**Table 2. Examples of field large-scale direct shear testing**

| Originator or Reference  | Shear box $L$ (cm) $\times$ $W$ (cm) $\times$ $T$ (cm)     | Material   |
|--------------------------|--|--|
| Marsland [43]            | $61 \times 61 \times 10$                                   | Stiff fissured clay  |
| O’loughlin & Pearce [44] | $31 \times 31 \times 15$                                   | Soil-siltstone interface on slope  |
| Endo [45]                | $50 \times 50 \times 25$                                   | Clay with roots, evaluating the impact of tree roots on soil shear strength    |
| Brand [46]               | $30 \times 30 \times 15$                                   | Residual soil and soft rock  |
| Matsuoka et al. [4]      | $122.5 \times 122.5 \times 16, 63.2 \times 63.2 \times 16$ | Coarse granular materials, including rockfill with max particle size of 300 mm |
| Fakhimi et al. [47]      | $75 \times 75 \times 35$                                   | Clayey sand with a trace of gravel at tunnel excavation area                   |
| Fakhimi et al. [48]      | $60 \times 60 \times 30, 30 \times 30 \times 30$           | By-product material from ore extraction (i.e., mine waste)                     |
| Oyanguren et al. [49]    | $120 \times 120 \times 52$                                 | Rockfill of Llerin Dam   |
| Zou et al. [50]          | $50 \times 50 \times 45$                                   | Sand-gravel in the Three Gorges Dam  |
| Sagnak et al. [6]        | $70 \times 70 \times 35$                                   | Metamorphic rocks in the foundation of Gölecik Dam                             |

The execution of direct shear test is generally simple. The test is initiated by preparing a geomaterial sample in a shear box (Figure 7). The sample has an initial height  $T$ , a length  $L$ , and a shear plane with a cross-section of  $A$ . The sample is given a vertical load of  $N$  which causes a normal confining stress of:

$$\sigma_n = N/A \quad (1)$$

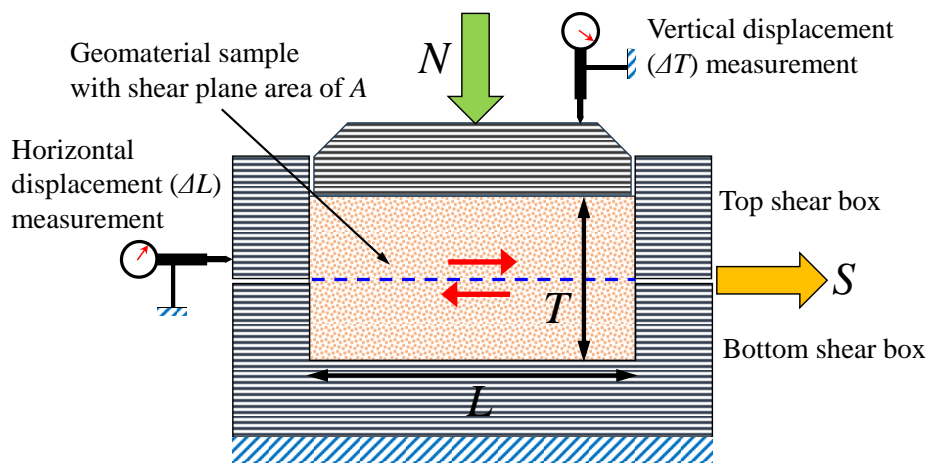


**Figure 7. General direct shear test configuration**

The normal stress value is held constant throughout the test duration. The subsequent step is shearing the sample.

There are 2 options for shearing the sample, namely strain and stress controlled. The strain-controlled method is carried out so that the value of the increase in shear strain ( $\delta$ ) or horizontal displacement ( $\Delta L$ ) that occurs in the sample is maintained. The strain control method can provide an opportunity to observe post-peak behavior in the variation between shear stress ( $\tau$ ) and shear strain. This method in certain conditions may provide distinctive peak strength. Alternatively, if the stress-controlled method is selected, the horizontal force ( $S$ ) or shear stress is applied in equal increments until failure occurs. According to Das [51], stress-controlled tests are likely to model the real field situation better than strain-controlled tests.

The horizontal force applied in the sample results in a shear stress equal to:

$$\tau = S/A \quad (2)$$

Shear strain is obtained from the ratio of horizontal deformation or displacement to the initial sample height, namely:

$$\delta = \Delta L/T \quad (3)$$

The axial strain value ( $\varepsilon$ ), which is the ratio of vertical displacement ( $\Delta T$ ) to the initial sample height, is calculated using the following equation:

$$\varepsilon = \Delta T/T \quad (4)$$

In each test, variations  $N$ ,  $S$ ,  $\Delta L$ , and  $\Delta T$  values are recorded against time synchronously. These parameters can be analyzed to obtain  $\sigma_n$ ,  $\tau$ ,  $\delta$ , and  $\varepsilon$ .

A series of direct shear tests are conducted using at least 3 similar geomaterial samples. Each sample is given a  $\sigma_n$  value that is different from the others. Accordingly, the variation of normal stress with maximum shear stress can be evaluated to obtain a failure model, for instance the Mohr-Coulomb or M-C failure model [52, 53].

## 5. Shear Strength of Random Material

Dam stability analysis demands reliable shear strength of random material, particularly when random material is placed in the main dam body. As random material comprises an extensive range of particle sizes, its shear strength mainly depends on the dominant material type and the composition. Okamoto [54] presented a summary of various shear strength failure models of geomaterials in dam engineering, including the linear M-C as well as non-linear power equation criteria that are commonly applied for random materials. The M-C model is regularly applied to common random materials that have a broad range of particle sizes or rich in fine grain particles. The power equation model is frequently recommended for random materials that are rich in large grain particles, including rockfill size materials. The selection of shear strength models for random material must be determined by the design engineer based on material type, design requirements, and data availability.

The Mohr-Coulomb line is considered as a well-known failure model for geomaterials and has a long history in geotechnical engineering practice. Equation (5) shows the shear strength of geomaterial ( $\tau_s$ ) based on the M-C model. This model uses 2 intrinsic parameters of soil shear strength, namely cohesion ( $c$ ) and angle of internal friction ( $\varphi$ ).

$$\tau_s = c + \sigma_n \tan(\varphi) \quad (5)$$

where  $\sigma_n$  is normal confining stress.

The shear strength of fine-grained soils, namely clay and silt, are normally related to the cohesion, as one of parameters in the M-C model. But granular geomaterials having negligible contents of fine-grained soils, such as rockfill, may still possess a significant cohesion value. Coduto [55] and Leps [56] described that high cohesion in granular materials is related to disguised frictional strength or apparent cohesion. According to Mitchell [57], dilation, apparent mechanical force, as well as negative pore water pressure are generally sources of the apparent cohesion. An example of apparent mechanical force is particle interlocking. In structural fill embankment, a compaction by heavy machinery normally leads to much better particle interlocking.

The linear M-C shear strength envelope practically can be used for all types of geomaterials. Nonetheless, the actual behavior of some geomaterials is extremely non-linear over a broad range of confining normal stress. The following power equation or parabolic model is commonly used to incorporate the non-linearity relationship between normal confining stress and shear strength.

$$\tau_s = A\sigma_n^b \quad (6)$$

where  $A$  and  $b$  are power equation fitting parameters. These parameters do not have physical meaning [28]. Marsal [58] and De Mello [59] were among the first who proposed this model for rockfill materials in dams. Since then, many authors have adopted this non-linear approach e.g., [60-64]. The non-linearity behavior of large particle geomaterials, such as rockfill, is associated with many reasons. For example, Muñiz-Menéndez & Estaire [40] described that this non-linearity may be attributed to grain breakages.

Hyperbolic model [65] was also applied for random material in addition to M-C and power models. For instance, Fu et al. [25] and Ferreira et al. [23] used hyperbolic model to evaluate stability of a core dam made of random material. The hyperbolic model demands parameters that are beyond the scope of this current study.



## 6. Application of ILSDS Test in Rukoh Dam

### 6.1. General

Zones with high risk of slope instability in Rukoh Dam were constructed using random fill materials. Evaluation of dam stability requires valid and reliable geomaterial shear strength. Geomaterial shear strength could be assessed in the field and the laboratory. However, common field and laboratory tests may not result in dependable shear strength values of random materials. This dependability concern is associated with the presence of large-sized grains. These large particles cannot be accommodated by regular laboratory sample size. If a regular-size device is used, testing can be addressed by scaling down the original field grain size distribution. Large particles are removed in such a way that the new grain size distribution is parallel to the field grain distribution [4]. Wang et al. [66] found that this approach could greatly influence the test outcome. The Japanese Geotechnical Society advised a minimum sample size for a triaxial test on material containing large particles, such as rockfill [67]. It is advised that the sample diameter test be at minimum 4 times the largest particle grain size [67]. Matsuoka et al. [4] as well as Wang et al. [5] confirmed the applicability of this recommendation for large-scale direct shear testing. Additionally, the laboratory testing cannot replicate the field compaction work's impact on the shear strength. Laboratory samples are commonly prepared using laboratory compactors that are different from the field compactors. Thus, these compaction methods do not have equivalent compaction energy.

IGI, ITB, and UTM developed an ILSDS device. This device generally adopted the theoretical approach of common laboratory direct shear equipment in evaluating the shear strength of a geomaterial. Nevertheless, the ILSDS test could provide shear strength appraisal of random material with large grains in the real compacted field conditions. This device was proposed by the authors for estimating the shear strength of compacted fill, such as random material, during construction of large dam projects in Indonesia. The device was capable of running a stress-controlled test. This apparatus was developed based on findings and suggestions from relevant previous studies, e.g., [4, 68, 69]. The main component of the ILSDS apparatus was a shear box having dimensions of  $70 \times 70 \times 30$  cm. The proposed test only required a single shear box, whereas the common direct shear device has top and bottom boxes. A set of pressure manometer cells and one set of vertical and horizontal displacement gauges were used in this method (Figure 8). A larger shear box with a shear plane of  $80 \times 80 \times 30$  cm thick was also available. All shear boxes were built using 1.5-cm-thick steel plates. One pair of 3-L capacity hydraulic pumps was utilized for manually applying the vertical and horizontal loads. These pumps were connected to their corresponding 1-MPa hydraulic jacks. The horizontal and vertical hydraulic jack stroke lengths were 26 cm and 15 cm, respectively. Seven lubricated cylindrical rollers with a diameter of 4.5 cm were placed in between the lower and upper top plates. The compacted random fill was excavated and carved to prepare at minimum 3 samples in a testing location.

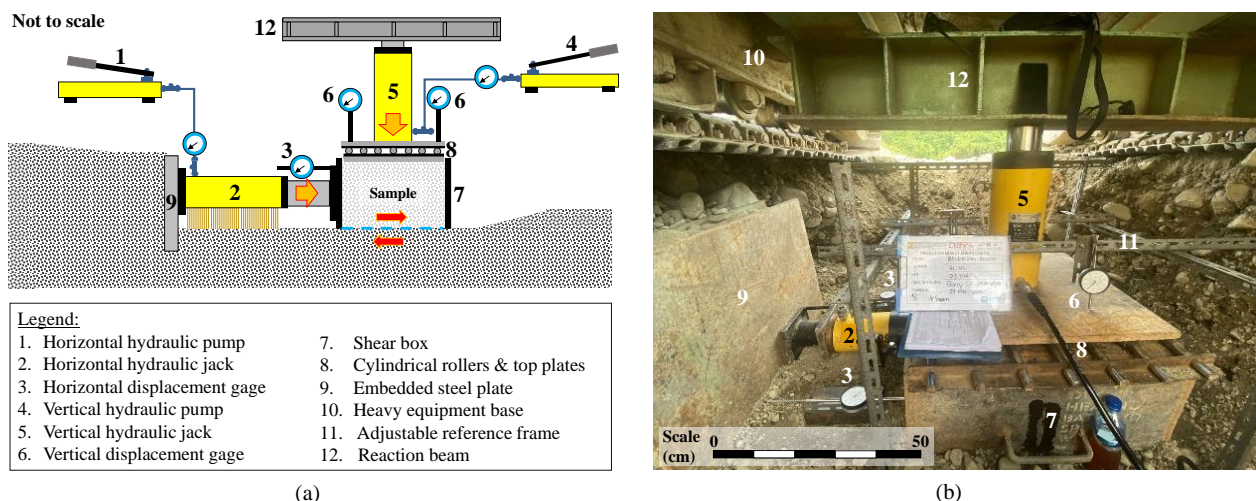


Figure 8. ILSDS test: (a) configuration and (b) execution

The ILSDS was employed for testing random materials in several large dam projects in Indonesia. This method was used in Semantok Dam [12]. Upon construction completion in 2022, this dam was considered the longest dam in the region of Southeast Asia. Hakim et al. [13] presented the ILSDS application in Keureuto Dam. Sahadewa [15] reported variability in shear strength of random material based on ILSDS tests in Kuwil Kawangkoan Dam.

## 6.2. Test Execution

A number of ILSDS tests were conducted for assessing random fill material shear strength in Rukoh Dam. Ten locations, A to J, at various stations and different elevations were selected for testing. These locations have been compacted by a vibratory roller during the construction stage. Random materials in Location C were disposal material from excavation works in Rukoh Dam. This location was used for a trial embankment to study the feasibility of excavated material. In the other testing locations, random materials were obtained from borrow areas.

The ILSDS tests in Rukoh Dam were performed using  $70 \times 70 \times 30$  cm shear boxes. In any testing site, 3 random material samples were arranged. The maximum normal confining stress ( $\sigma_{n-max}$ ) in a testing location was calculated based on the corresponding final overburden load. Testing preparation was initiated by conducting excavation (Figure 9-a). The excavation depth and width were set in such a way that the ILSDS test could be performed using an excavator for vertical reaction. Subsequently, a top plate was placed at the excavation surface as a template for sample preparation (Figure 9-b). Hand tools, such as a shovel, hoe, and handspike, were used to manually carve the sample (Figure 9-c). Afterwards, a shear box was installed in each sample (Figure 9-d). The top plate was removed to flatten the sample surface (Figure 9-e). The lower top plate was placed on the sample (Figure 9-f).

Thereafter, cylindrical rollers and an upper top plate were installed. Afterwards, an embedded steel plate was set in place using an excavator (Figure 10-a). This steel plate served as a horizontal reaction. Then, a set of reaction beams was installed on top of a vertical hydraulic jack using an excavator (Figure 10-b). The measuring devices and adjustable reference frames were arranged similar to the testing setup shown in Figure 8 and Figure 10-c. An excavator was positioned above the testing location for providing the vertical reaction (Figure 10-d). Afterwards, the first random material sample was loaded with a normal confining stress of one-third  $\sigma_{n-max}$  using the vertical hydraulic jack. The normal stress value was kept stable in the remaining testing duration. Shearing or horizontal loading was not applied on the sample until no further significant settlement occurred (i.e., 2 consecutive readings showed settlement less than 0.05 mm). An increasing horizontal load of 50 kPa/minute in the pressure manometer was assigned to the random material sample via the horizontal hydraulic jack until failure. During testing, the load and displacement values were recorded at an incremental time. The other samples were tested similarly under different and larger normal vertical stresses (i.e., two-thirds  $\sigma_{n-max}$  and  $\sigma_{n-max}$ ). A flowchart showing the test methodology is presented in Figure 11.



**Figure 9. Sample preparation: (a) pit excavation, (b) top plate for template, (c) manual carving, (d) shear box placement, (e) surface sample flattening, and (f) lower top plate installation**





**Figure 10. Field test setup: (a) steel plate horizontal reaction, (b) reaction beam installation, (c) hydraulic jack, reference frame, and measuring device installations, and (d) excavator alignment**

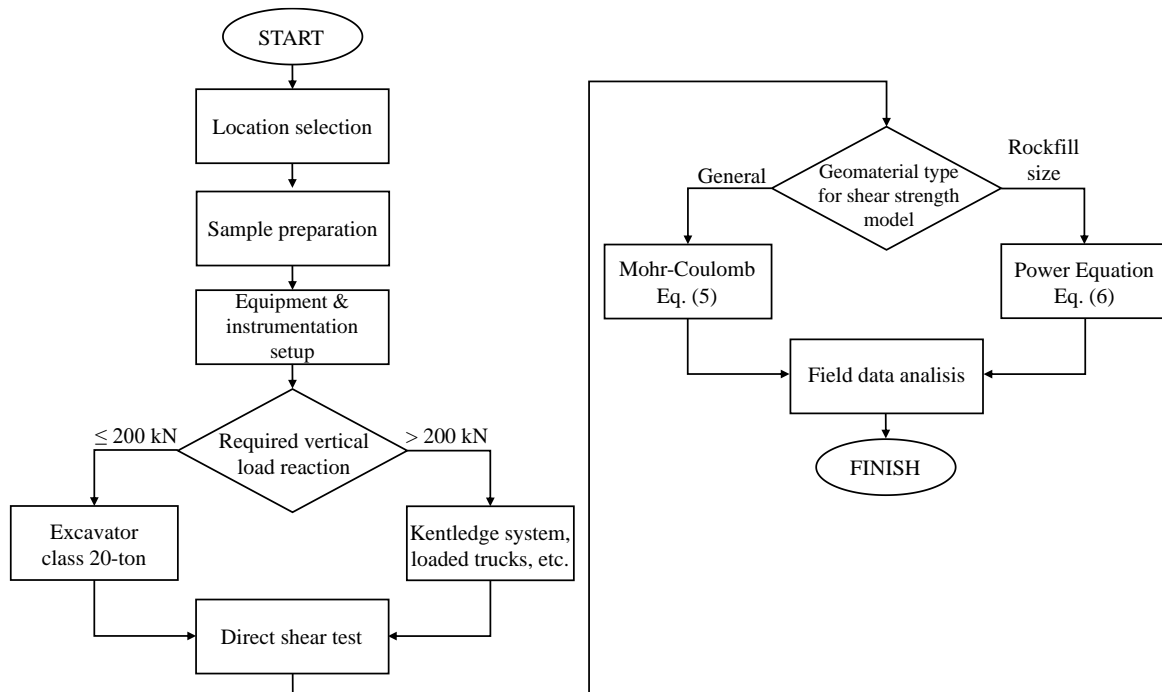


**Figure 11. Flowchart showing the ILSDS methodology**

A series of field and laboratory tests for evaluating material properties of compacted random fill was performed using samples around the ILSDS testing locations by other parties. The ring water replacement method was performed to measure the in situ compacted density of random fill. Random material samples were collected for laboratory testing, including grain size analysis and other index property tests. The field and laboratory test results that were provided to the authors are compiled in Table 3, including void ratio ( $e$ ) as well as water content ( $w$ ). The available grain size distribution ranges are shown in Figure 12. This figure suggests that random materials in Rukoh Dam were practically within the size limits of rockfill materials. Although the random materials in Rukoh Dam could be classified as rockfill material based on grain size, these materials were still considered and treated as random materials in the entire project.

This type of geomaterial is commonly designated as random rockfill or random rock material in Indonesia. Random rockfill material collection in Rukoh Dam was not controlled nor inspected as strictly as that of rockfill. For example, the random materials were not passed through rigorous tests, including abrasion, rock soundness, slaking durability, and compressive strength tests. Visual field observation suggested that random materials in Rukoh Dam were dominated by andesite rocks in various degrees of weathering.

**Table 3. Sample characteristics and properties of random materials in Rukoh Dam**

| Location * | Compacted dry density (kN/m <sup>3</sup> ) |      |      | Relative density (%) |      |       | <i>e</i> |       |       | <i>w</i> (%) |      |      |
|------------|--|------|------|----------------------|------|-------|----------|-------|-------|--------------|------|------|
|            | Min  | Ave. | Max  | Min                  | Ave. | Max   | Min      | Ave.  | Max   | Min          | Ave. | Max  |
| A          | 20.4                                       | 22.9 | 23.9 | 89.4                 | 94.1 | 98.6  | 0.115    | 0.155 | 0.268 | 0.51         | 1.11 | 1.44 |
| D          | 20.5                                       | 23.0 | 24.0 | 87.2                 | 97.3 | 105.9 | 0.106    | 0.150 | 0.290 | 0.46         | 0.79 | 1.54 |
| E          | 20.3                                       | 21.7 | 23.8 | 51.5                 | 86.5 | 97.2  | 0.118    | 0.216 | 0.292 | 0.26         | 0.77 | 1.98 |
| F          | 21.7                                       | 23.0 | 23.9 | 90.2                 | 98.7 | 104.7 | 0.111    | 0.148 | 0.205 | 0.46         | 0.96 | 1.39 |
| G          | 22.9                                       | 23.4 | 23.7 | 81.8                 | 90.2 | 96.0  | 0.122    | 0.138 | 0.160 | 0.48         | 0.76 | 1.13 |
| H          | 23.0                                       | 23.6 | 23.8 | 83.9                 | 93.5 | 98.6  | 0.115    | 0.129 | 0.154 | 0.35         | 0.80 | 1.36 |
| I          | 23.5                                       | 23.7 | 23.9 | 92.6                 | 95.7 | 99.0  | 0.114    | 0.123 | 0.131 | 0.40         | 0.47 | 0.55 |
| J          | 23.1                                       | 23.4 | 23.6 | 85.2                 | 89.9 | 93.6  | 0.128    | 0.138 | 0.151 | 0.15         | 0.72 | 1.15 |

\* Data from Location B and C were not available to the authors.

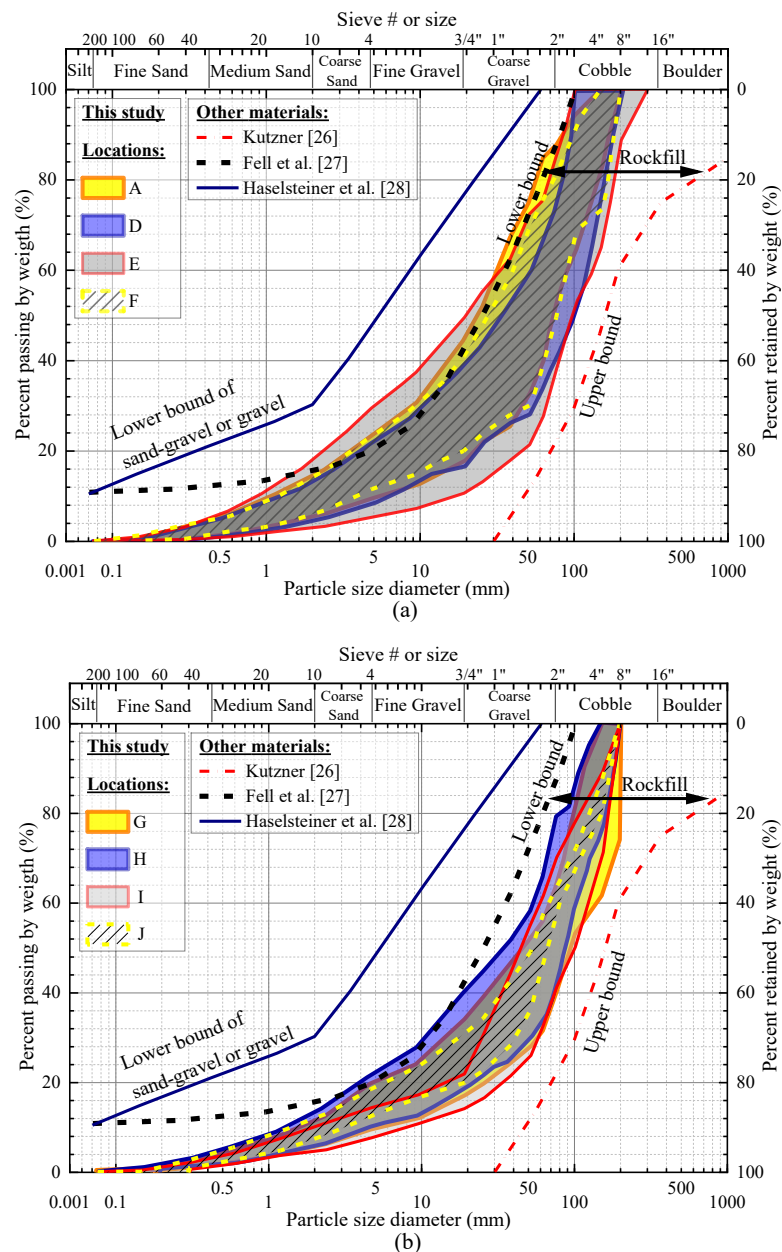


**Figure 12. Particle size distribution samples around Location: (a) A to F and (b) G to J**



### 6.3. Test Result

The ILSDS test results from locations A to J are presented in Figures 13 to 17. These figures show the relationships among vertical-horizontal displacements and shear stress under 3 different normal stresses. In Location A, the peak shear strength increased from 123 kPa to 292 kPa as the normal stresses increased from 96 kPa to 283 kPa. The variation between horizontal and vertical displacements displayed volume change behavior of the sample. In Location A, this relationship exhibited compressive or contractive behavior of the random material samples at low horizontal displacement or initial shearing. At larger horizontal displacements until failure, dilative behavior occurred. The variation between vertical and horizontal displacements in Location A is a typical behavior of dense granular soil. In general, testing from the other locations exhibits similar results to that of Location A. First, the peak shear stress raised with the normal stresses. Second, the samples commonly experienced contraction at small horizontal displacement and dilated at higher horizontal displacement. Nevertheless, Location C resulted in variation between shear stress and vertical-horizontal displacements that was different from the general trend observed in other locations. In Location C, no distinctive peak nor shear strength plateau was observed in the variation between horizontal load and shear stress. The shear strength was determined using the shear stress value that corresponded with 10% relative lateral displacement ( $\Delta L/L$ ) as suggested by ASTM D3080/D3080M-23 [70].

Additionally, samples in Location C always experienced contractive behavior during shearing under all normal stresses. There are 2 possible explanations for this behavior. First, this contractive behavior is commonly demonstrated by loose granular soil. Visual observation suggested that random materials in Location C were dominated by sandy materials with fine-grain particles. Even small rockfill-sized materials were barely found in this location. Although no in-situ density test results in Location C were provided to the authors, it was reported that the trial embankment compaction in this location was performed by 6 passes of a heavy compactor per lift layer. The other testing locations were compacted by 8 passes. Hence, the random material in Location C was likely loose or less dense than that of the other locations. Second, the contractive behavior may be related to grain breaking under the corresponding confining normal stress. The samples would have exhibited dilative behavior during shearing load application if the grain particles lasted unbroken under the confining normal stress. At confining normal stress that is relatively large to the material, the dilative behavior is inhibited by the normal stress. The random materials in Location C were collected from excavation disposal, whereas the other locations' random materials were borrowed from areas out of the project area. In the end, the random materials in Location C were not utilized for Rukoh Dam construction.

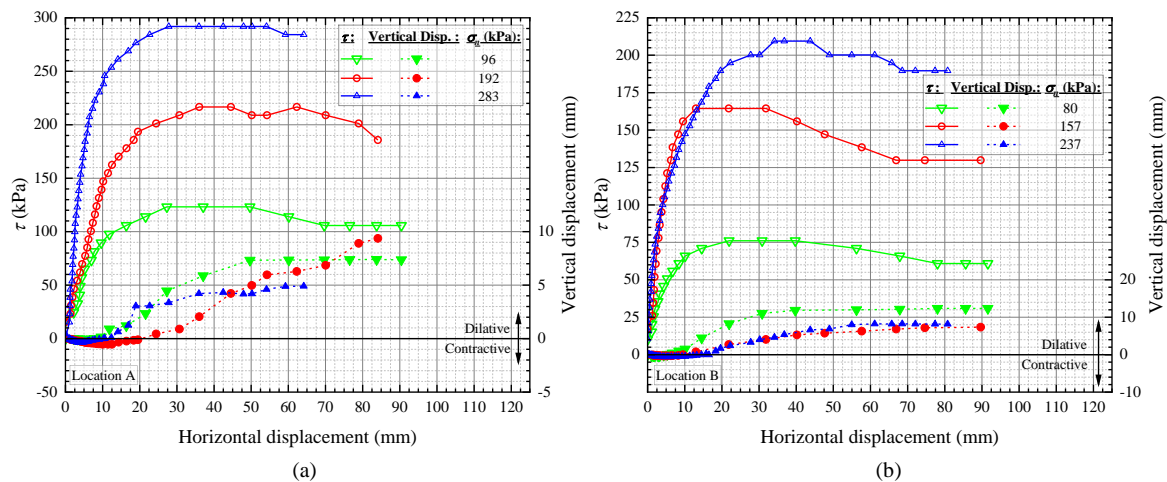


Figure 13. ILSDS results in Location: (a) A and (b) B

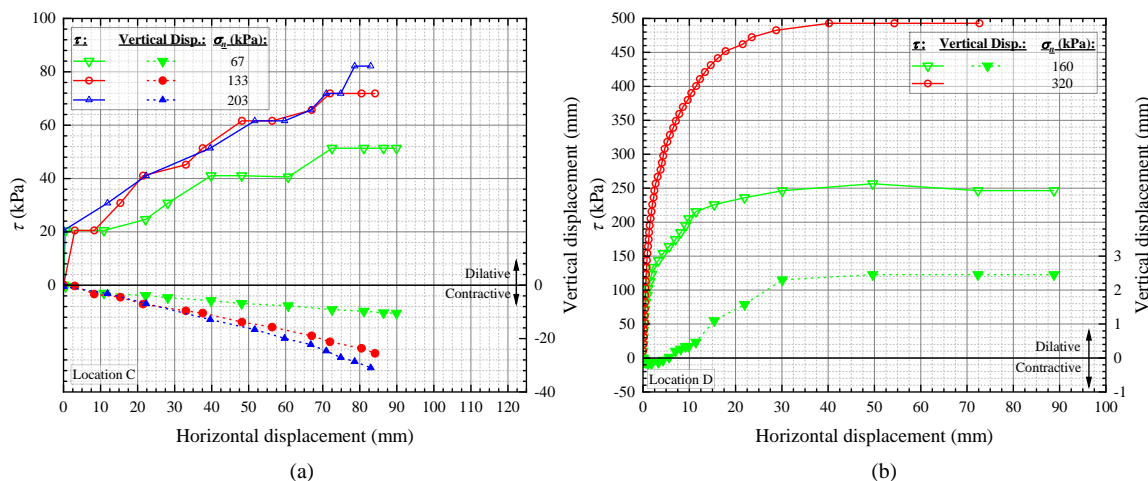


Figure 14. ILSDS results in Location: (a) C and (b) D

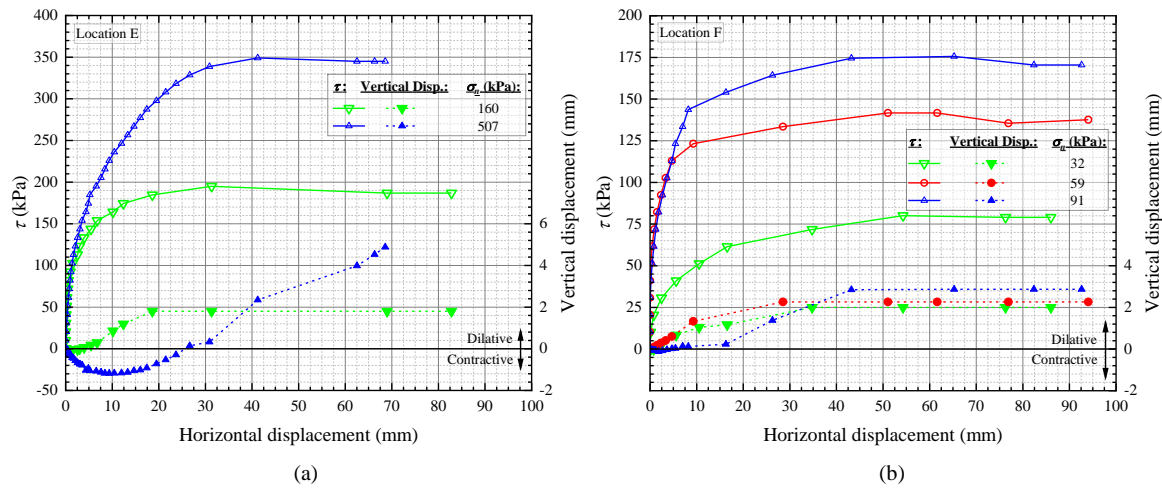


Figure 15. ILSDS results in Location: (a) E and (b) F

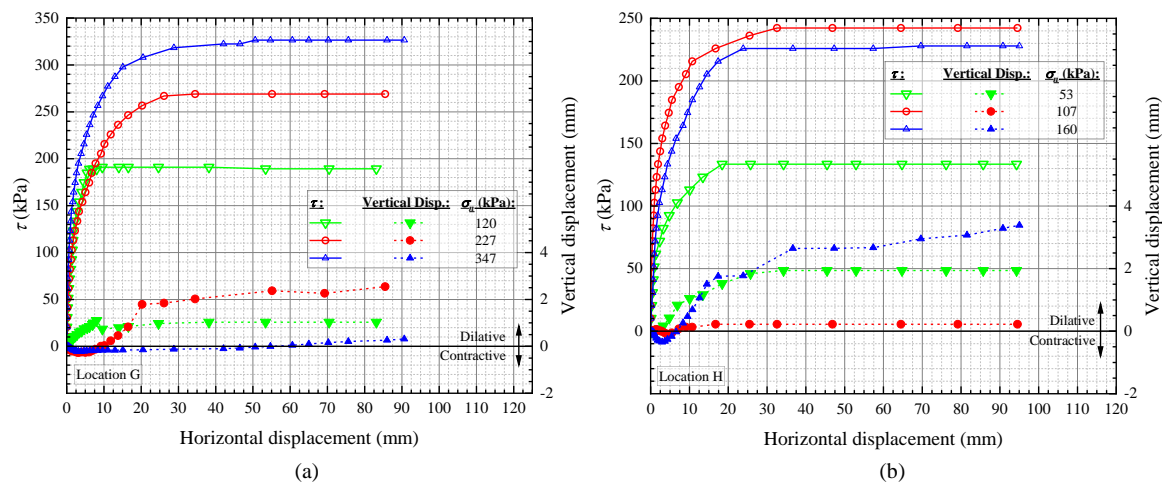


Figure 16. ILSDS results in Location: (a) G and (b) H

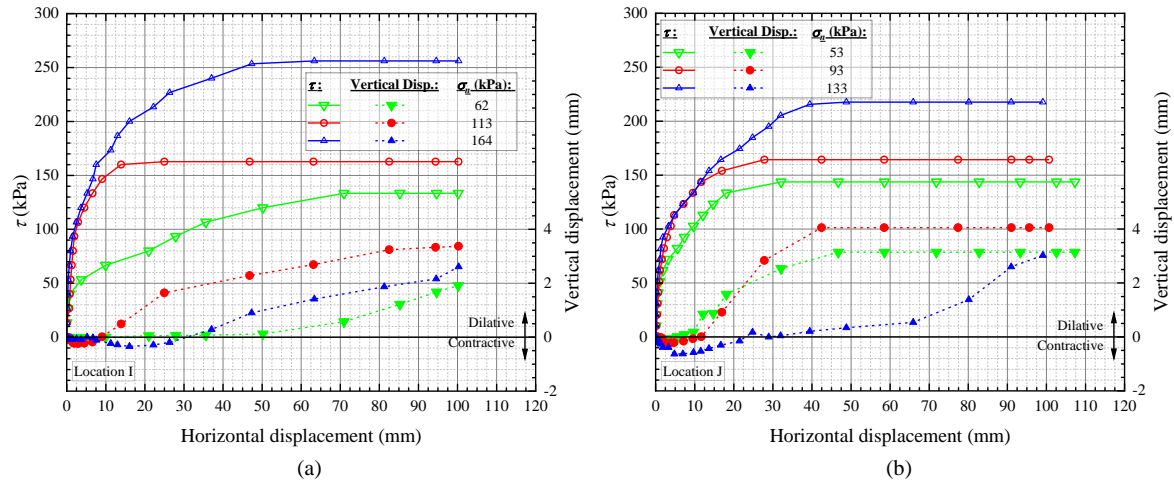


Figure 17. ILSDS results in Location: (a) I and (b) J

Several problems occurred in performing testing in Locations D and E. In Location D sample 2, the vertical displacement measurements were unreliable. This issue may be attributed to the unstable condition of the adjusted reference frame for holding the vertical displacement measurement. Although the relationship between horizontal and vertical displacements was not acquired, the shear strength of this sample could still be obtained. During testing of sample 3 in Location D, the embedded steel plate for horizontal reaction was accidentally shifted, leading to useless shear load and horizontal displacement data. Sample 2 in Location E also had a similar issue. These 2 samples were excluded from this study.

The testing results from all locations under normal stress, varying from 32 to 507 kPa, are summarized in Table 4. This table also shows lateral and vertical displacements at failure. If the failure point was not obvious, the shear stress

at 10% relative lateral displacement was taken as failure [70], such as failure determination in Location C. Failure for random rock materials on average was 37.8 mm and varied from 13.9 mm to 70 mm. In terms of relative lateral displacements, these values were 5.4% on average and ranged from 2% to 10%. The vertical displacement of random rockfill at failure varied from 0.2 mm to 11 mm with an average value of 2.5 mm. The secant friction angle ( $\phi_s$ ) of random rockfill ranged from 34.6° to 68.2° with a mean value of 55.22°. These secant friction angles were calculated by assuming a zero  $c$ -value in the M-C line for each sample. The highest  $\phi_s$  value from this study was still lower than the highest  $\phi_s$  value of 70° from open-graded aggregate materials containing particles larger than 25 mm as reported by Nicks et al. [71].

**Table 4. Summary of ILSDS test results**

| Location | Sample | Normal stress,<br>$\sigma_n$ (kPa) | Shear strength,<br>$\tau_s$ (kPa) | Lateral displacement,<br>$\Delta L$ , at failure (mm) | Vertical Displacement,<br>$\Delta T$ , at failure (mm) | Secant friction angle,<br>$\phi_s$ (°) | Max dilation<br>angle, $\psi_{\max}$ (°) |
|----------|--------|------------------------------------|-----------------------------------|---|--|--|--|
| A        | 1      | 96                                 | 123                               | 37.1  | 5.9  | 52                                     | 20.3                                     |
|          | 2      | 192                                | 217                               | 36.0  | 2.1  | 48.4                                   | 14.3                                     |
|          | 3      | 283                                | 292                               | 27.3  | 3.4  | 45.9                                   | 41.6                                     |
| B        | 1      | 80                                 | 76                                | 30.8  | 11.0   | 43.5                                   | 33.8                                     |
|          | 2      | 157                                | 164                               | 21.9  | 2.7  | 46.3                                   | 12.4                                     |
|          | 3      | 237                                | 209                               | 36.8  | 5.4  | 41.4                                   | 29.2                                     |
| C        | 1      | 67                                 | 49                                | 70.0  | -9.0   | 36.3                                   | -  |
|          | 2      | 133                                | 69                                | 70.0  | -18.0  | 27.4                                   | -  |
|          | 3      | 203                                | 71                                | 70.0  | -38.0  | 19.2                                   | -  |
| D        | 1      | 160                                | 257                               | 49.6  | 2.5  | 58                                     | 9.1                                      |
|          | 2      | 320                                | 493                               | 40.2  | -  | 57                                     | -  |
|          | 3      | -                                  | -                                 | -   | -  | -                                      | -  |
| E        | 1      | 160                                | 195                               | 31.3  | 1.8  | 50.7                                   | 9.4                                      |
|          | 2      | -                                  | -                                 | -   | -  | -                                      | -  |
|          | 3      | 507                                | 349                               | 41.2  | 2.4  | 34.6                                   | 11.0                                     |
| F        | 1      | 32                                 | 81                                | 54.3  | 2.0  | 68                                     | 8.4                                      |
|          | 2      | 59                                 | 142                               | 51.1  | 2.3  | 67                                     | 9.0                                      |
|          | 3      | 91                                 | 175                               | 43.2  | 2.9  | 63                                     | 8.4                                      |
| G        | 1      | 120                                | 189                               | 13.9  | 0.8  | 57.6                                   | 17.4                                     |
|          | 2      | 227                                | 269                               | 34.5  | 2.0  | 49.9                                   | 14.4                                     |
|          | 3      | 347                                | 327                               | 46.5  | 0.2  | 43.3                                   | 0.6                                      |
| H        | 1      | 53                                 | 134                               | 25.7  | 1.8  | 68.2                                   | 11.2                                     |
|          | 2      | 107                                | 242                               | 32.6  | 0.2  | 66.2                                   | 4.2                                      |
|          | 3      | 160                                | 226                               | 23.9  | 1.8  | 54.7                                   | 13.0                                     |
| I        | 1      | 62                                 | 133                               | 70.0  | 0.6  | 65.2                                   | 1.3                                      |
|          | 2      | 113                                | 163                               | 25.0  | 1.7  | 55.2                                   | 6.0                                      |
|          | 3      | 164                                | 256                               | 63.4  | 0.9  | 57.3                                   | 3.4                                      |
| J        | 1      | 53                                 | 143                               | 32.1  | 2.5  | 68.2                                   | 15.4                                     |
|          | 2      | 93                                 | 164                               | 27.8  | 2.8  | 60.4                                   | 10.0                                     |
|          | 3      | 133                                | 217                               | 48.8  | 0.3  | 58.5                                   | 5.6                                      |

The relationship between horizontal and vertical displacements is presented in Figures 13 to 17, including random rockfill that exhibited dilative behavior during shearing. This dilative behavior is commonly described by the ratio of vertical to horizontal displacements ( $\Delta T/\Delta L$ ). The dilation angles during testing generally fluctuated. Nicks et al. [71] also reported fluctuation of dilation angles during testing. The maximum angle of dilation ( $\psi_{\max}$ ) of the random rockfill samples is presented in Table 4. The average  $\psi_{\max}$  value was 12.9°, which varied from 0.6° to 41.6°. This fluctuation may be attributed to various sources, including grain particle size, shape, density, compressive strength, and confining stress in the random rock materials. According to Lee & Seed [72], at high confining stress, the dilation mechanism diminishes greatly. Grain particle crushing under this high confining stress tends to result in contraction behavior.

The peak shear stress-normal stress relationship was obtained by evaluating the variation among shear stress, normal confining stress, and horizontal displacement in 10 locations (Figure 18). In each location, if possible, this variation was regressed using the M-C line and power equation models. M-C line regression was performed if at least 2 data points in a location were available. The power equation regression was conducted if 3 data points in a location were available. Based on M-C models shown in Figure 18-a, the cohesion value varied between 16.1 to 124.3 kPa. This cohesion had an average of 62.8 kPa as well as a standard deviation of 41.5 kPa. The  $\phi$  values of the M-C line varied from  $9^\circ$  to  $58.4^\circ$ . This angle of internal friction had a mean value and standard deviation of  $39.8^\circ$  and  $15^\circ$ , respectively. Figure 18-b shows the power equation model for each location. The  $A$  parameter was on average 10.32 and ranged from 1.36 to 17.98 with a standard deviation of 6.47. The  $b$  parameter ranged from 0.346 to 0.927 with a standard deviation of 0.192 and a mean of 0.628. Figure 18-b also suggests that the power equation models were within the shear strength limits for rockfill proposed by Barton [73] and Leps [56]. This figure also presents shear strength rock categories from very weak to strong as proposed by Haselsteiner et al. [28]. According to this category, the shear strength of random material in Location B was categorized as very weak to weak. The shear strength of Location A was designated between weak to medium. Shear strength models of locations F, I, and J fell within medium to strong. The shear strength in Location G at low confining normal stress was categorized as medium to strong. At higher normal stress, it shifted from the weak to the medium category. Then, at even higher normal stress, it translated to very weak to medium. Location H was practically categorized as medium to strong. In Location C, random material shear strength was below the lower bound for rockfill. This result agreed with the visual observation showing that random materials in Location C were dominated by sand and fine-grained particles that were much smaller than rockfill. Figure 18 implies that there is high variability of shear strength in terms of M-C and power equation models. The M-C and power equation model parameters of 10 locations are summarized in Table 5.

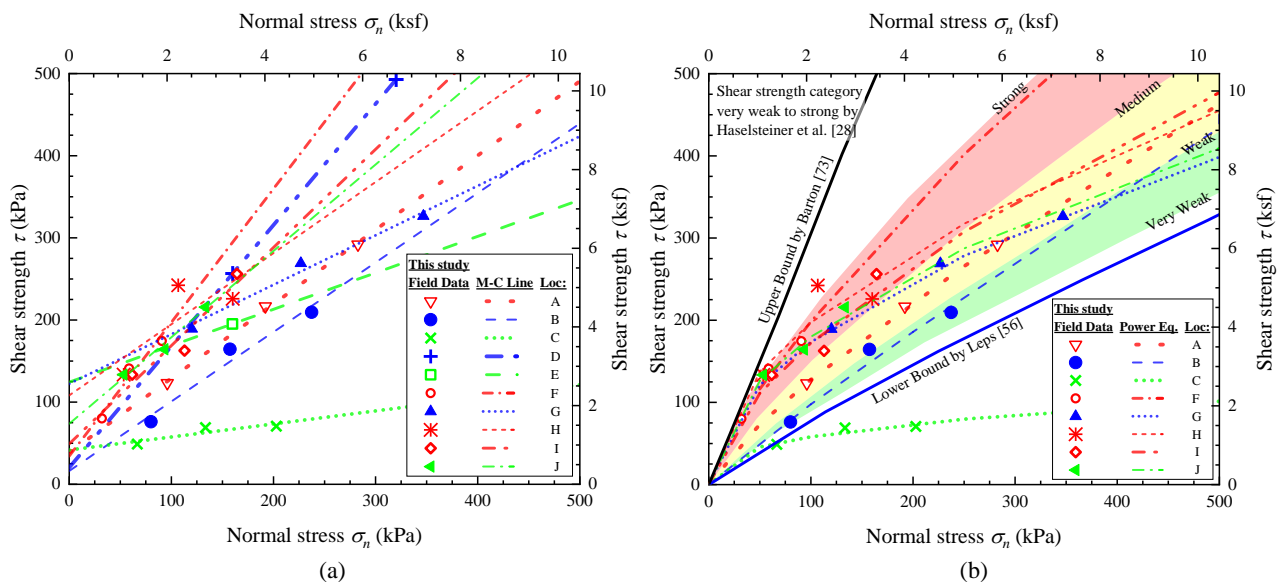


Figure 18. Shear strength models: (a) M-C and (b) power equation

Table 5. Shear strength parameters

| Location | Mohr-Coulomb |                     | Power equation ( $\tau$ , and $\sigma_n$ in kPa) |       |
|----------|--------------|---------------------|--|-------|
|          | $c$ (kPa)    | $\phi$ ( $^\circ$ ) | $A$  | $b$   |
| A        | 38.5         | 42.1                | 3.19   | 0.801 |
| B        | 16.1         | 40.2                | 1.363  | 0.927 |
| C        | 41.6         | 9                   | 11.77  | 0.346 |
| D        | 20.3         | 55.9                | -  | -     |
| E        | 124.3        | 23.9                | -  | -     |
| F        | 34.2         | 58.4                | 5.71   | 0.770 |
| G        | 122.3        | 31.1                | 16.03  | 0.517 |
| H        | 108.2        | 40.9                | 17.98  | 0.519 |
| I        | 49.1         | 50.1                | 9.34   | 0.633 |
| J        | 73.6         | 46.4                | 17.15  | 0.510 |

The size of random materials in Rukoh Dam resembled that of rockfill (Figure 12). In Indonesia, this random material is commonly designated as random rockfill or random rock. The secant friction angle from this study was compared with the general correlation between secant friction angle of granular materials and normal stress for various initial void ratios ( $e_0$ ) proposed by Terzaghi et al. [74]. This comparison is presented in Figure 19. Terzaghi et al. [74] developed



this relationship based on a database of triaxial tests on sand, gravel, and larger alluvial particles of strong massive mineral as well as rocks. Rockfill grades from A to E based on unconfined compressive strength (UCS) are also presented in Figure 19. Terzaghi et al. [74] comprised secant friction angle values as high as  $60^\circ$  at low confining stress. But at low confining stress, the secant friction angle can reach above  $70^\circ$ , as shown by Nicks et al. [71]. The current study and Terzaghi et al. [74] similarly indicated that the secant friction angle declined with confining stress. But the secant friction angle change with confining normal stress of this study was generally more sensitive than that of Terzaghi et al. [74]. It is interesting to see that some data points, at normal confining stresses below 200 kPa from this study, were above recommendations from Terzaghi et al. [74]. These data points were associated with a field initial void ratio that was as low as 0.11 (Table 3). This void ratio was higher than the available highest void ratio of 0.2 in Terzaghi et al. [74]. Furthermore, it is also understood if the  $\phi$  value of the direct shear test is commonly larger than that of the triaxial test [71]. Data from Location C generally corresponded with recommendations from Terzaghi et al. [74] for high void ratio and below the lowest rockfill grade. This condition apparently suggested that random material in Location C was likely less dense than that of the other locations.

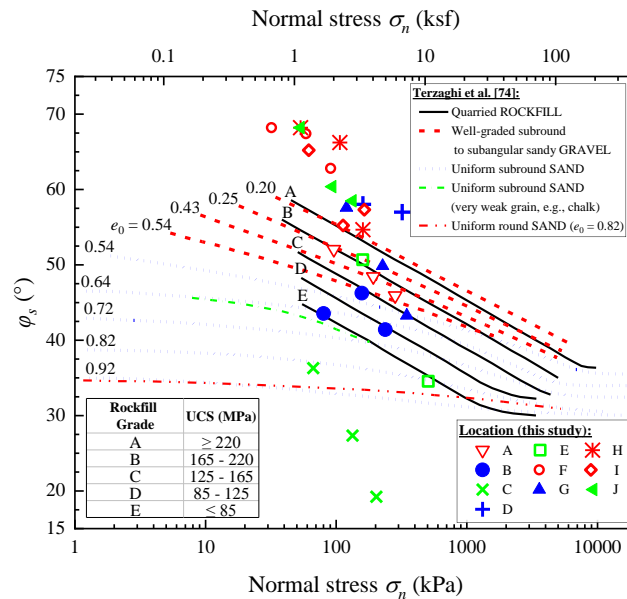


Figure 19. Relationship between normal stress and secant friction angle

A dependency in the  $A$  and  $b$  values of the power equation parameters is observed in this study (Figure 20). This finding is consistent with previous rockfill shear strength studies by Haselsteiner et al. [28] and Muñoz-Menéndez & Estaire [40]. The  $A$  and  $b$  values depended on the units in which the shear and normal stresses were expressed [75]. Non-dimensional units in the power equation relationship could be made by normalizing the unit in the normal and shear stresses using atmospheric pressure. Thus, the correlation is more physically accepted. Nevertheless, as shown by Muñoz-Menéndez & Estaire [40], if the power equation relationship was derived using the unit of shear and normal stresses (i.e., kPa), the relationship between  $A$  and  $b$  was much less scattered. The utilization of this unit optimized significantly the correlation between the 2 parameters.

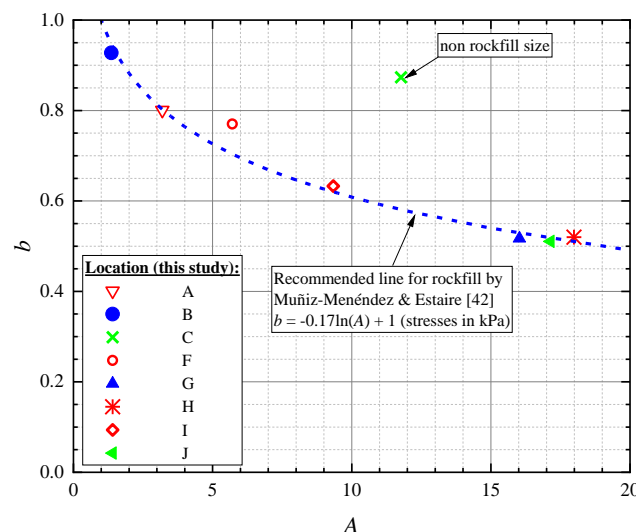


Figure 20. Relationship between  $A$  and  $b$  parameters of the power equation (stresses in kPa)

Muñiz-Menéndez & Estaire [40] formed a database containing approximately 100 large-scale tests on rockfill samples from CEDEX, Laboratorio de Geotecnia, Madrid, Spain, and from the literature over 4 decades. Based on this database, Muñiz-Menéndez & Estaire [40] developed a correlation between  $A$  and  $b$  parameters to verify the validity of test results (Figure 20). The proposed correlation for verification purposes is presented in Equation 7. This equation was derived using the unit of shear and normal stresses in kPa. In this figure,  $A$  and  $b$  parameters from testing in Rukoh Dam show a very good agreement with Muñiz-Menéndez & Estaire [40]. This agreement highlights the validity of the ILSDS test for material with large particles. Additionally, it can be seen that the test result from Location C was above the verification line. As previously explained, samples in Location C were sandy materials with fine particle contents and exhibited different behaviors from those of other locations.

$$b = -0.17 \cdot \ln(A) + 1 \text{ (stresses in kPa)} \quad (7)$$

#### 6.4. Large-Scale Shear Strength Test Recommendation Based on ILSDS Test

Random materials have been successfully utilized in numerous large dam projects in the world. This success, at least partly, came from controlling and verifying the properties and content of the random materials themselves. Unfortunately, due to the authors' dam project experiences, the "Random" term in random material has been mistakenly comprehended. In field execution, a variety of geomaterials can be incorrectly introduced to random materials just to reach the required volume. Potential danger may arise due to this practice. First, problematic geomaterials (i.e., expansive soil, organic soil, low slaking durability materials, etc.) may enter the random materials. Second, it also introduces even larger variability and complexity in many engineering properties of random material, including the shear strength.

The ILSDS test for evaluating dam embankment material's shear strength is highly recommended, particularly if the material contains large-sized particles. This field shear strength test is reliable, fast, practical, and economical. The ILSDS test was introduced after the X Dam failure, when the other large dam projects in Indonesia were in the construction stage. The ILSDS test was developed mainly for evaluating and verifying shear strength of compacted fill material on site. This test was designed to utilize equipment and machinery that were readily available in a dam construction. In addition to applying large-scale tests in the construction stage, it is also crucial to utilize this test in the pre-construction stage. Many benefits can be obtained by performing the pre-construction testing approach. In the pre-construction stage, the ILSDS test in a trial embankment can serve to evaluate the feasibility of random material samples from the borrow areas or quarries. It can also assess the performance of the proposed compaction work method. In the construction phase, the ILSDS test serves as shear strength verification that incorporates field compaction work performance. This testing result can confirm if the field shear strength values fulfill the design values or not. Thus, it can be considered if the design and construction compaction method should be modified or if they could proceed directly. In this case, if the field shear strength is lower than the design values, the dam project team can mitigate this issue by reducing embankment slope inclination, changing to better fill materials, and improving the compaction procedure. The number of ILSDS can be proposed depending on the shear strength results in the pre-construction stage and the designer's confidentiality.

Laboratory large-scale shear strength tests can be performed to assess material feasibility as an alternative in the pre-construction stage. While the ILSDS test can capture shear strength spatial variability between testing locations, this test itself is not ideal to find specific material properties behind this variability during construction. If a shear strength parametric study is needed, the laboratory large-scale test is preferable to the ILSDL test. Performing a set of material property tests prior to the shear strength test in the laboratory is more controllable and convenient than performing the corresponding test in the field.

The large-scale direct shear testing should be accompanied by other geomaterial properties tests if this information is of interest. For example, geomaterial properties tests can be used to avoid problematic materials. Common geomaterial testing, such as sieve analysis, natural water content, specific gravity, and relative density, should be performed on random material samples. If it is deemed necessary, large particles of random materials should also be tested specifically, including abrasion, rock soundness, slaking durability, and compressive strength tests. These large grain particle tests are important to completely evaluate their behavior, including grain breakage and durability potentials that influence the shear strength of random materials.

## 7. Summary, Conclusion and Suggestion

Zoned embankment dams commonly include random fill materials in particular zones. These random material zones significantly impact the dam stability. The shear strength of random material plays a vital role in dam stability analysis. Regrettably, it is difficult to reliably evaluate the shear strength. Furthermore, it is challenging to find literature about the shear strength of this material. IGI, ITB, and UTM were in collaboration to devise large-scale direct shear or ILSDS equipment to test dam construction material on site. The ILSDS test was designed to use equipment and machinery that were immediately available in a dam construction. This method was successfully applied to assess random fill in 10 locations of Rukoh Dam, Indonesia.

The ILSDS test is a compelling approach for assessing random fill material on site. This method could capture volume change behavior of random material during shearing. This direct shear test was capable of showing whether the geomaterial failed in contraction or dilation. In addition, the effect of field compaction work on the shear strength can also be assessed using this method. The ILSDS test results in Rukoh Dam emphasized the necessity of random material shear strength appraisal. Test results suggested high spatial variability in shear strength of random materials as indicated by the M-C model and power equation parameters.

Random materials in Rukoh Dam could be considered as random rockfill according to the particle size distribution. The ILSDS test results were compared with results from relevant studies for rockfill. Terzaghi et al.'s [74] recommendation on secant friction angle showed similar patterns with this study, namely that secant friction angle decreases with confining stress. But this current study shows a more rapid decrease. A recommendation line to represent the relationship between  $A$  and  $b$  in the power equation as proposed by Muñiz-Menéndez and Estaire [40] was also compared. The results of this current study were generally consistent with the recommendation line by Muñiz-Menéndez and Estaire [40]. This agreement emphasizes the validity of the current study.

The ILSDS test on random material is reliable, rapid, simple, and inexpensive. It is strongly recommended as part of the mandatory routine in the construction stages of a dam project, particularly if the material contains large grain particles and is placed in dam failure-prone zones. Although the ILSDS test was mainly developed for shear strength verification in the construction stage, this test can also be conducted in the pre-construction stage. In the pre-construction stage, it can be performed in a trial embankment to choose suitable and feasible quarry or borrow areas. The in-situ pre-construction test in the trial embankment is also advised to evaluate field compaction work performance. If an area for trial embankment is not available, a large-scale laboratory shear strength test can be conducted as an alternative for selecting appropriate materials. In addition, the laboratory test can also be performed for a parametric study on material shear strength. In the construction stage, the in situ large-scale method offers verification of the shear strength of compacted material. The testing result could confirm if shear strength values already meet the requirements or not. Therefore, it can be concluded whether the design and construction compaction method have to be modified or if they can be proceeded further. The large-scale testing should be accompanied by other geomaterial property tests, including sieve analysis, natural water content, specific gravity, and relative density to avoid problematic materials. In addition, abrasion, rock soundness, slaking durability, and compressive strength tests should also be performed on the large particles in random materials.

## 8. Declarations

### 8.1. Author Contributions

Conceptualization, A.S. and A.M.H.; methodology, A.S., A.M.H., and H.E.S.; formal analysis, A.S.; investigation, A.S. and A.M.H.; resources, A.S., A.M.H., and H.E.S.; data curation, A.S., A.M.H., and H.E.S.; writing—original draft preparation, A.S.; writing—review and editing, A.S. and A.M.H.; visualization, A.S.; supervision, S.A.K. and S.K.; project administration, A.S. and A.M.H.; funding acquisition, A.S. All authors have read and agreed to the published version of the manuscript.

### 8.2. Data Availability Statement

The data presented in this study are available on request from the corresponding author.

### 8.3. Funding

This study was financially sponsored by Bandung Institute of Technology or Institut Teknologi Bandung (ITB) through Program Pengabdian Masyarakat dan Inovasi (PPMI) or Community Service and Innovation Scheme year 2025 (Project ID: FTSL.PPMI-2025).

### 8.4. Acknowledgements

This article was written based on an Indonesian Geotechnical Institute's study. The authors would like to express gratitude to ITB for financially supporting this study. The authors would be grateful to acknowledge Ibadurrahman Adz Dzikro and Hana Yasmin Kamila of ITB for their support. The authors also would appreciate extending their gratitude to Banyu Bumi Sangkara's support in field testing execution that played a crucial role in this research. Any findings, conclusions, opinions, and suggestions written in this article belong to the authors. They may not automatically describe the thought of the supporting institutions.

### 8.5. Conflicts of Interest

The authors declare no conflict of interest.

## 9. References

- [1] Sánchez-Martín, J., Galindo, R., Arévalo, C., Menéndez-Pidal, I., Kazanskaya, L., & Smirnova, O. (2020). Optimized Design of Earth Dams: Analysis of Zoning and Heterogeneous Material in Its Core. *Sustainability* (Switzerland), 12(16), 6667. doi:10.3390/su12166667.
- [2] Sahadewa, A., Setyawan, H., Tanjung, M., Pamumpuni, A., Hakim, A. M., Langit, J., Herry, P., & Wibowo, A. (2022). Construction Failure of X Dam: The Importance of Field Monitoring. 11<sup>th</sup> International Symposium of Field Monitoring in Geomechanics, 4-8 September, 2022, London, United Kingdom.
- [3] Liu, S. H. (1999). Development of a New Direct Shear Test and Its Application to the Problems of Slope Stability and Bearing Capacity. PhD Thesis, Nagoya Institute of Technology, Nagoya, Japan.
- [4] Matsuoka, H., Liu, S., Sun, D., & Nishikata, U. (2001). Development of a New In-Situ Direct Shear Test. *Geotechnical Testing Journal*, 24(1), 92–102. doi:10.1520/gtj11285j.
- [5] Wang, J. J., Zhang, H. P., Wen, H. B., & Liang, Y. (2015). Shear Strength of an Accumulation Soil from Direct Shear Test. *Marine Georesources and Geotechnology*, 33(2), 183–190. doi:10.1080/1064119X.2013.828821.
- [6] Sagnak, M., Işık, N. S., Cüceoğlu, F., Aydın, S., & Koçbay, A. (2024). Investigation of In-Situ Shear Strength Parameters in Gölecik Dam Foundation, Bursa, Türkiye. ENGCEO'2024, National Symposium on Engineering Geology and Geotechnics, 6-8 June, 2024, Nevşehir, Turkey.
- [7] Zhang, X., Ji, S., Feng, Y., Li, Y., & Zhao, C. (2025). A Comparison on the Effects of Coal Fines and Sand Fouling on the Shear Behaviors of Railway Ballast Using Large Scale Direct Shear Tests. *Journal of Traffic and Transportation Engineering (English Edition)*, 12(1), 52–67. doi:10.1016/j.jtte.2022.09.003.
- [8] Wang, J.-Q., Zhang, T.-Y., Dong, C.-F., & Tang, Y. (2025). Quantifying Railway Ballast Degradation through Repeated Large-Scale Direct Shear Tests and Three-Dimensional Morphological Analysis. *International Journal of Geomechanics*, 25(4), 10252. doi:10.1061/ijgnai.gmeng-10252.
- [9] Hassan, M. O., Jafari, N. H., Twilley, R. R., & Rovai, A. S. (2024). Large-Scale Laboratory Direct Shear Testing for Wetland Root Strength. *Geo-Congress 2024*, 370–376. doi:10.1061/9780784485330.038.
- [10] Chao, Z., Fowmes, G., Mousa, A., Zhou, J., Zhao, Z., Zheng, J., & Shi, D. (2024). A New Large-Scale Shear Apparatus for Testing Geosynthetics-Soil Interfaces Incorporating Thermal Condition. *Geotextiles and Geomembranes*, 52(5), 999–1010. doi:10.1016/j.geotextmem.2024.06.002.
- [11] Chen, J. F., Liu, Z. N., Gu, Z. A., Zhu, Y., & Gao, J. L. (2024). Large-Scale Direct Shear Test of the Interface Between Coral Sand and Geogrid. *Applied Ocean Research*, 153, 104219. doi:10.1016/j.apor.2024.104219.
- [12] Sahadewa, A. (2023). Case History of Random Material Shear Strength Evaluation using In-situ Large Scale Direct Shear Test in the Construction of the Longest Dam in the Southeast Asian. *IOP Conference Series: Earth and Environmental Science*, 1249(1), 12011. doi:10.1088/1755-1315/1249/1/012011.
- [13] Hakim, A. M., Kamaruddin, S. A., Sahadewa, A., Nazir, R., & Setyawan, H. E. (2023). Effect of Grain Size Distribution on Shear Strength Characteristic of Random Fill Material at Keureuto Dam, Indonesia. *Key Engineering Materials*, 970, 151–156. doi:10.4028/p-h30laq.
- [14] Sahadewa, A. (2023). In Situ Large Scale Direct Shear Test for Evaluating Compaction Work of Random Material: Case of Construction Failure in an Indonesia Dam. *Key Engineering Materials*, 972, 125–132. doi:10.4028/p-28QzdB.
- [15] Sahadewa, A. (2024). The Spatial Variability of Random Fill Shear Strength Based on In-Situ Large Scale Direct Shear Test in the Kuwil Kawangkoan Dam Construction. *Proceedings of 6<sup>th</sup> International Conference on Civil Engineering and Architecture*, Vol. 1. ICCEA 2023, Lecture Notes in Civil Engineering, 530, Springer, Singapore. doi:10.1007/978-981-97-5311-6\_14.
- [16] United States Bureau of Reclamation (USBR). (2012). Design Standards No. 13: Embankment Dams (Chapter 2: Embankment Design Phase 4 [Final]. United States Department of the Interior, Bureau of Reclamation, Denver, United States.
- [17] United States Society on Dams (USSD). (2011). Materials for Embankment Dams. United States Society on Dams, Denver, United States.
- [18] International Commission on Large Dams (ICOLD). (1989). Moraine as Embankment and Foundation Material - State of the Art, Bulletin 69. International Commission on Large Dams, Paris, France.
- [19] Sherard, J. L., & Dunnigan, L. P. (1989). Critical Filters for Impervious Soils. *Journal of Geotechnical Engineering*, 115(7), 927–947. doi:10.1061/(ASCE)0733-9410(1989)115:7(927).
- [20] Rönnqvist, H. (2010). Predicting Surfacing Internal Erosion in Moraine Core Dams. Ph.D. Thesis, Royal Institute of Technology (KTH), Stockholm, Sweden.
- [21] Bernell, L. (1982). Experiences of Wet Compacted Dams in Sweden. 14<sup>th</sup> International Congress on Large Dams, 3-7 May, 1982, Rio de Janeiro, Brazil.



- [22] Xu, Z., & Jiang, G. (2017). Technologies on Construction of Earth Core Rockfill Dams. *Revista Brasileira de Engenharia de Barragens*, 5, 42-54.
- [23] Ferreira, B. S., Almeida, M. S. S., Lopes, F. R., Reis Cavalcanti, M. do C., & Pires Filho, C. J. (2022). On the Use of Random Material in Dam Cores: Case of the Manso Dam, Brazil. *Geotechnical and Geological Engineering*, 40(4), 1973–1987. doi:10.1007/s10706-021-02003-7.
- [24] Ma, H., & Chi, F. (2016). Major Technologies for Safe Construction of High Earth-Rockfill Dams. *Engineering*, 2(4), 498–509. doi:10.1016/J.ENG.2016.04.001.
- [25] Fu, Z., Chen, S., Ji, E., Li, G., & Lu, Y. (2020). Using Clay-Gravel Mixtures as the Impervious Core Materials in Rockfill Dams. *Dam Engineering - Recent Advances in Design and Analysis*, Chapter 1. IntechOpen, London, United Kingdom. doi:10.5772/intechopen.93206.
- [26] Kutzner, C. (1996). *Earth and Rockfill Dams for Reservoirs*. Ferdinand Enke Verlag, Stuttgart, Germany. (In German).
- [27] Fell, R., MacGregor, P., Stapledon, D., & Bell, G. (2005). *Geotechnical Engineering of Dams* (1<sup>st</sup> Ed.). CRC Press, London, United Kingdom. doi:10.1201/NOE0415364409.
- [28] Haselsteiner, R., Pamuk, R., & Ersoy, B. (2017). Aspects Concerning the Shear Strength of Rockfill Material in Rockfill Dam Engineering. *Geotechnik*, 40(3), 193–203. doi:10.1002/gete.201600099.
- [29] Hoeg, K., Fell, R., & Bridle, R. (2012). BC Hydro WAC Bennett Dam: Expert Engineering Panel Report No. N3405, Volumes 1 and 2, BC Hydro, Vancouver, Canada.
- [30] Rönqvist, H., & Viklander, P. (2015). Applying Empirical Methods to Assess the Internal Stability of Embankment Dam Cores of Glacial Till. *Geomaterials*, 5(1), 1–18. doi:10.4236/gm.2015.51001.
- [31] Boudia, A., Berga, A., Boudia, S., & Hussain, S. K. (2021). The Detailed Study on the Development of the Triaxial Equipment in the Soil Mechanics: A Review. *International Journal of Multidisciplinary Research and Growth Evaluation*, 2(6), 67–76. doi:10.54660/anfo.
- [32] Skempton, A. W. (1949). Alexandre Collin a Note on His Pioneer Work in Soil Mechanics. *Geotechnique*, 1(4), 215–222. doi:10.1680/geot.1949.1.4.215.
- [33] Skempton, A. W. (1958). Arthur Langtry Bell (1874-1956) and His Contribution to Soil Mechanics. *Geotechnique*, 8(4), 143-157. doi:10.1680/geot.1958.8.4.143.
- [34] Matthews, M. C. (1988). Engineering Application of Direct and Simple Shear Testing. *Ground Engineering*, 21(2), 13–21.
- [35] Bowles, J. (1992). *Engineering Properties of Soil and Their Measurements*. 4<sup>th</sup> Edition, McGraw-Hill, Boston, United States.
- [36] Davies, M. C. R., & Le Masurier, J. W. (1997). Soil/Nail Interaction Mechanisms from Large Direct Shear Tests. *Ground Improvement Geosystems Densification and Reinforcement: Proceedings of the Third International Conference on Ground Improvement Geosystems*, 3-5 June, 1997, London, United Kingdom.
- [37] Andjelkovic, V., Pavlovic, N., Lazarevic, Z., & Radovanovic, S. (2018). Modelling of Shear Strength of Rockfills Used for the Construction of Rockfill Dams. *Soils and Foundations*, 58(4), 881–893. doi:10.1016/j.sandf.2018.04.002.
- [38] Tanghetti, G., Goodey, R. J., Divall, S., McNamara, A. M., & McKinley, B. (2019). Design and Development of a Large Shear Box for Testing Working Platform Material. *XVII European Conference on Soil Mechanics and Geotechnical Engineering*, 1-6 September, 2019, Reykjavik, Iceland.
- [39] Srivastava, L. P., Singh, M., & Singh, J. (2019). Development of Large Direct Shear Test Apparatus for Passive Bolt Reinforced Mass. *Indian Geotechnical Journal*, 49(1), 124–131. doi:10.1007/s40098-018-0306-6.
- [40] Muñoz-Menéndez, M., & Estaire, J. (2022). Experimental Study on the Shear Strength of Medium-Coarse Rockfill. *Proceedings from the 20th International Conference on Soil Mechanics and Geotechnical Engineering*, 1-5 May, 2022, Sydney, Australia.
- [41] Attom, M. F. (1997). The Effect of Compactive Energy Level on Some Soil Properties. *Applied Clay Science*, 12(1–2), 61–72. doi:10.1016/S0169-1317(96)00037-3.
- [42] Yamin, M., Attom, M. F., Atabay, S., & Vandanapu, R. (2021). The Effect of Compaction Effort on Shear Strength Parameters of Low/High Plasticity Clay Soils. *Geotechnical Engineering*, 52(2), 1–8. doi:10.14456/seagj.2021.32.
- [43] Marsland, A. (1971). The Use of In-Situ Tests in a Study of the Effects of Fissures on the Properties of Stiff Clays. *Proceedings of the First Australian–NZ Conference on Geomechanics*, 9-13 August, 1971, Melbourne, Australia.
- [44] O’Loughlin, C. L., & Pearce, A. J. (1976). Influence of Cenozoic Geology on Mass Movement and Sediment Yield Response to Forest Removal, North Westland, New Zealand. *Bulletin of the International Association of Engineering Geology*, 13(1), 41–46. doi:10.1007/BF02634757.

- [45] Endo, T. (1980). Effects of Tree Roots upon Shear Strength of Soil. *Japan Agricultural Research Quarterly*, 14(2), 112–115.
- [46] Brand, E. W. (1985). Predicting the Performance of Residual Soil Slopes. *Proceedings of the 11<sup>th</sup> International Conference on Soil Mechanics and Foundation Engineering*, Vol. 5, 2541–2578, A.A. Balkema, Rotterdam, the Netherlands.
- [47] Fakhimi, A., Salehi, D., & Mojtabai, N. (2004). Numerical Back Analysis for Estimation of Soil Parameters in the Resalat Tunnel Project. *Tunnelling and Underground Space Technology*, 19(1), 57–67. doi:10.1016/S0886-7798(03)00087-7.
- [48] Fakhimi, A., Boakye, K., Sperling, D. J., & McLemore, V. T. (2008). Development of a Modified In Situ Direct Shear Test Technique to Determine Shear Strength Parameters of Mine Rock Piles. *Geotechnical Testing Journal*, 31(3), 269–273. doi:10.1520/gtj101152.
- [49] Oyanguren, P. R., Nicieza, C. G., Fernández, M. I. Á., & Palacio, C. G. (2008). Stability Analysis of Llerin Rockfill Dam: An In Situ Direct Shear Test. *Engineering Geology*, 100(3–4), 120–130. doi:10.1016/j.enggeo.2008.02.009.
- [50] Zou, Z., Zhang, Q., Xiong, C., Tang, H., Fan, L., Xie, F., Yan, J., & Luo, Y. (2020). In Situ Shear Test for Revealing the Mechanical Properties of the Gravelly Slip Zone Soil. *Sensors (Switzerland)*, 20(22), 1–16. doi:10.3390/s20226531.
- [51] Das, B. M. (2009). *Principles of Geotechnical Engineering* (7<sup>th</sup> Ed.). CL Engineering, Boston, United States.
- [52] Coulomb, C. A. (1776). Essay on an Application of the Rules of Maximis and Minimis to Some Problems of Statics, Relating to Architecture. *Memoires de Mathematique de l'Academie Royale de Science*, 7, 343–387. (In French).
- [53] Mohr, O. (1900). What Conditions Determine the Elastic Limit and Fracture of a Material?. *Zeitschrift des Vereins Deutscher Ingenieure*, 44(45), 1524–1530. (In German).
- [54] Okamoto, T. (2004). Evaluation of In-Situ Strength of Rockfill Material Taking into Account of In-Situ Density and Strength by Laboratory Test. *Proceedings of the 4th International Conference on Dam Engineering - New Developments in Dam Engineering*, 18–20 October, 2004, Nanjing, China.
- [55] Coduto, D. P. (2014). *Foundation Design: Principles and Practices*. Pearson Education Limited, London, United Kingdom.
- [56] Leps, T. M. (1970). Review of Shearing Strength of Rockfill. *Journal of the Soil Mechanics and Foundations Division*, 96(4), 1159–1170. doi:10.1061/jsfeaq.0001433.
- [57] Mitchell, J. K. (1993). *Fundamentals of Soil Behavior* (2<sup>nd</sup> Ed.). John Wiley & Sons, Hoboken, United States.
- [58] Marsal, R. J. (1973). *Mechanical Properties of Rockfill*. John Wiley & Sons, Hoboken, United States.
- [59] De Mello, V. F. B. (1977). Reflections on Design Decisions of Practical Significance to Embankment Dams. *Geotechnique*, 27(3), 281–355. doi:10.1680/geot.1977.27.3.281.
- [60] Indraratna, B. (1994). Implications of Non-Linear Strength Criteria in the Stability Assessment of Rockfill Dams. *International Conference on Soil Mechanics and Foundation Engineering*, 5–10 January, 1994, New Delhi, India.
- [61] Estaíre, J., & Olalla, C. (2006). Analysis of the Strength of Riprap using Direct Shear Tests in a 1 × 1 m<sup>2</sup> Box. *Ingeniería Civil*, 144, 73–79. (In Spanish).
- [62] Frossard, E., Hu, W., Dano, C., & Hicher, P. Y. (2012). Rockfill Shear Strength Evaluation: A Rational Method Based on Size Effects. *Geotechnique*, 62(5), 415–427. doi:10.1680/geot.10.P.079.
- [63] Barton, N. (2013). Shear Strength Criteria for Rock, Rock Joints, Rockfill and Rock Masses: Problems and Some Solutions. *Journal of Rock Mechanics and Geotechnical Engineering*, 5(4), 249–261. doi:10.1016/j.jrmge.2013.05.008.
- [64] Ovalle, C., Frossard, E., Dano, C., Hu, W., Maiolino, S., & Hicher, P. Y. (2014). The Effect of Size on the Strength of Coarse Rock Aggregates and Large Rockfill Samples Through Experimental Data. *Acta Mechanica*, 225(8), 2199–2216. doi:10.1007/s00707-014-1127-z.
- [65] Duncan, J. M., & Chang, C.-Y. (1970). Nonlinear Analysis of Stress and Strain in Soils. *Journal of the Soil Mechanics and Foundations Division*, 96(5), 1629–1653. doi:10.1061/jsfeaq.0001458.
- [66] Wang, J.-J., Zhang, H.-P., Tang, S.-C., & Liang, Y. (2013). Effects of Particle Size Distribution on Shear Strength of Accumulation Soil. *Journal of Geotechnical and Geoenvironmental Engineering*, 139(11), 1994–1997. doi:10.1061/(asce)gt.1943-5606.0000931.
- [67] The Japanese Society of Soil Mechanics and Foundation Engineering. (1982). *Testing and Design Strength of Rockfill Materials*. The Japanese Society of Soil Mechanics and Foundation Engineering, Tokyo, Japan. (In Japanese).
- [68] Liu, S.-H. (2009). Application of In Situ Direct Shear Device to Shear Strength Measurement of Rockfill Materials. *Water Science and Engineering*, 2(3), 48–57. doi:10.3882/j.issn.1674-2370.2009.03.005.
- [69] Wang, J. J., Yang, Y., & Chai, H. J. (2016). Strength of a Roller Compacted Rockfill Sandstone from In-Situ Direct Shear Test. *Soil Mechanics and Foundation Engineering*, 53(1), 30–34. doi:10.1007/s11204-016-9360-1.

- [70] ASTM D3080/D3080M-23. (2023). Standard Test Method for Direct Shear Test of Soils Under Consolidated Drained Conditions. ASTM International, Pennsylvania, United States. doi:10.1520/D3080\_D3080M-23.
- [71] Nicks, J. E., Gebrenegus, T., & Adams, M. T. (2015). Strength Characterization of Open-Graded Aggregates for Structural Backfills, No. FHWA-HRT-15-034, Bureau of Transportation Statistics, U.S. Department of Transportation, Washington, United States.
- [72] Lee, K. L., & Seed, H. B. (1967). Drained Strength Characteristics of Sands. *Journal of the Soil Mechanics and Foundations Division*, 93(6), 117–141. doi:10.1061/jsfeaq.0001048.
- [73] Barton, N. (2008). Shear Strength of Rockfill, Interfaces and Rock Joints, and Their Points of Contact in Rock Dump Design. *Proceedings of the First International Seminar on the Management of Rock Dumps, Stockpiles and Heap Leach Pads*, 3-17. doi:10.36487/acg\_repo/802\_1.
- [74] Terzaghi, K., Peck, R. B., & Mesri, G. (1996). *Soil Mechanics in Engineering Practice*. John Wiley & Sons, Hoboken, United States.
- [75] Indraratna, B., Haque, A., & Aziz, N. (1999). Shear Behaviour of Idealized Infilled Joints Under Constant Normal Stiffness. *Geotechnique*, 49(3), 331–355. doi:10.1680/geot.1999.49.3.331.